Free Radical Biology and Medicine xxx (xxxx) 1–19

Contents lists available at ScienceDirect

Free Radical Biology and Medicine

journal homepage: www.elsevier.com/locate/freeradbiomed

Indole lactic acid derived from *Akkermansia muciniphila* activates the aryl hydrocarbon receptor to inhibit ferroptosis in ischemic stroke

Jiahan Wang [a, 1], Yongzheng Peng [b, 1], Yarui Liu [a], Zhuoshi Lian [a], Zheng Cai [a], Ye Chen [c], Haoqing He [a], Meilin Yang [a], Jie Zhao [a, bd, *]

[a] NMPA Key Laboratory for Research and Evaluation of Drug Metabolism, Guangdong Provincial Key Laboratory of New Drug Screening, School of Pharmaceutical Sciences, Southern Medical University, Guangzhou, 510515, China
[b] Department of Transfusion Medicine, Zhujiang Hospital, Southern Medical University, Guangzhou, 510282, China
[c] Department of Gastroenterology, Integrative Clinical Microecology Center, Shenzhen Hospital, Southern Medical University, Shenzhen, 518100, China
[d] Microbiome Medicine Center, Department of Laboratory Medicine, Zhujiang Hospital, Southern Medical University, Guangzhou, 510280, China

ARTICLE INFO

Keywords:
Akkermansia muciniphila
Indole lactic acid
Ischemic stroke
Aryl hydrocarbon receptor
Ferroptosis
Synbiotic

ABSTRACT

Ischemic stroke concurrent with gut microbiome dysbiosis induces intestinal damage, which exacerbates cerebral infarction. Probiotic or prebiotic interventions that reverse gut microbiome dysbiosis can promote recovery after ischemic stroke. *Akkermansia muciniphila* (AKK) safeguards intestinal health and is a promising probiotic; however, its role in ischemic stroke remains unclear. In this study, we found that live AKK, but not pasteurized AKK, mitigated ischemic-stroke-induced neurological injury, reduced cerebral infarction, and enhanced both blood-brain and intestinal barrier integrity. Moreover, the AKK supernatant reduced intestinal and cerebral injury, demonstrating efficacy comparable to that of live AKK. Metabolomic analysis revealed that the AKK supernatant was significantly enriched in indole lactic acid (ILA), a tryptophan metabolite. ILA levels were elevated in the serum and brains of pseudo-germ-free stroke rats administered AKK. Exogenous gavage with ILA mitigated ischemic-stroke-induced brain and intestinal damage. Mechanistically, ILA activated the aryl hydrocarbon receptor (AhR) and the nuclear transcription factor Nrf2, leading to the upregulation of SLC7A11 and GPX4 protein expression. This attenuated lipid peroxidation and intracellular iron accumulation triggered by ischemic stroke. Notably, intervention with the AhR inhibitor CH223191 abrogated the protective effects of ILA in ischemic stroke rats. These findings suggest that the therapeutic efficacy of AKK in ischemic stroke is at least partially attributable to ILA-mediated ferroptosis inhibition via AhR activation. AKK was selectively enriched by *Puerariae lobatae* Radix-resistant starch (PRS), promoting ILA generation more effectively than inulin and β-glucan. AKK and PRS synergistically alleviated ischemic-stroke-induced impairments, outperforming monomicrobial or prebiotic treatment alone. These findings reveal the unique mechanisms of AKK in ischemic stroke and provide a viable strategy for the clinical treatment of ischemic stroke through a novel synbiotic combination.

1. Introduction

Ischemic stroke is defined as a cerebral dysfunction caused by the narrowing or blockage of arteries that supply blood to the brain [1]. Due to its high incidence, disability rate, and mortality rate, stroke has become a major global public health challenge [2]. The pathogenesis of ischemic stroke is highly complex. Upon ischemia, insufficient ATP and glucose levels impair normal cellular metabolism [3]. This disruption leads to anaerobic metabolism, resulting in mitochondrial dysfunction, which further triggers oxidative stress, sterile inflammation, neurotoxic excitability, and other pathological processes that ultimately culminate in cell death within the ischemic region [4,5]. Cerebrovascular recanalization is the principal strategy for treating ischemic stroke. However, once blood flow and oxygen supply are restored, the body undergoes an oxidative stress response, generating reactive oxygen species (ROS). These ROS damage ferritin and mitochondria, leading to iron release that drives the Fenton reaction and ultimately results in lipid peroxidation and ferroptosis [6]. This cascade results in neuronal injury during

* Corresponding author. Department of Transfusion Medicine, Zhujiang Hospital, Southern Medical University, Guangzhou, 510282, China.
E-mail addresses: wangjiah954@163.com (J. Wang), yzpeng1981@126.com (Y. Peng), liuyarui_sandy@163.com (Y. Liu), zhuoshi_lian0818@163.com (Z. Lian), caizheng2002@sina.com (Z. Cai), chenye_2013@163.com (Y. Chen), hhq222888@163.com (H. He), mlyyyy2@163.com (M. Yang), zhaojie_0412@163.com (J. Zhao).
[1] These authors contributed equally to this work.

https://doi.org/10.1016/j.freeradbiomed.2025.04.020
Received 2 January 2025; Received in revised form 13 April 2025; Accepted 14 April 2025
0891-5849/

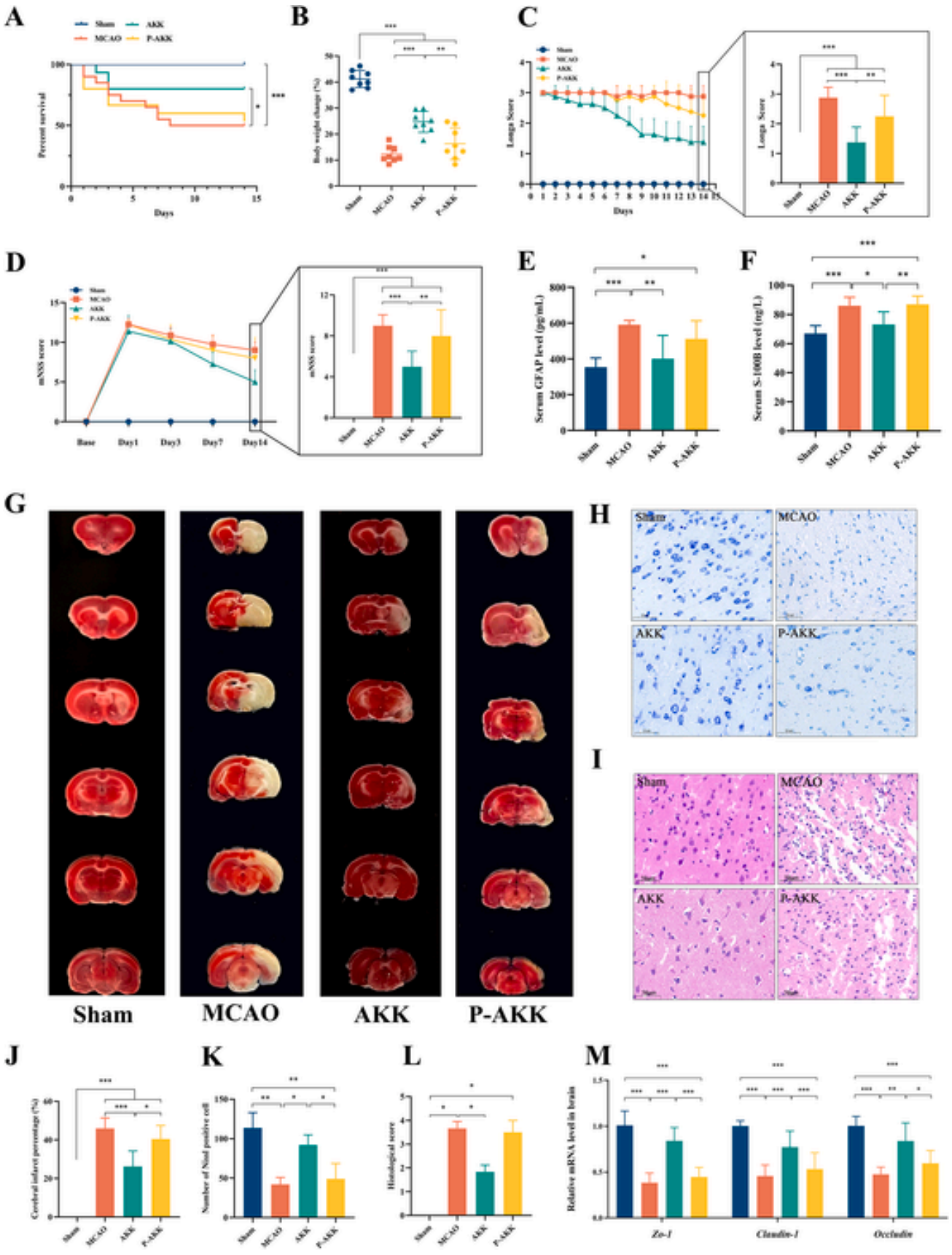
A
Sham
MCAO
AKK
P-AKK
Percent survival
Days
B
Body weight change (%)
C
Longa Score
Days
D
mNSS score
Base
Day1
Day3
Day7
Day14
E
Serum GFAP level (pg/mL)
F
Serum S-100B level (ng/L)
G
Sham
MCAO
AKK
P-AKK
H
I
J
Cerebral infarct percentage (%)
K
Number of Nissl positive cell
L
Histological score
M
Relative mRNA level in brain
Zo-1
Claudin-1
Occludin

Fig. 1. Live AKK gavage ameliorates brain injury in rats with ischemic stroke. (A) Survival curve. (Sham group n = 8 MCAO group n = 20 AKK group n = 15P-AKK group n = 15) (B) Relative body weight gain for 14 days. (C) Longa score. (D) mNSS score. (B-D n = 8). (E–F) Serum level of GFAP and S100B (n = 6). (G) Representative images of TTC staining (n = 4–5). (H) Representative images of Nissl staining (scale bar = 100 μm). (I) Representative micrographs of HE staining in the brain (× 200, scale bar = 100 μm). (J) Quantitative analysis of cerebral infarct areas (n = 4–5). (K) Quantification of the Nissl staining (n = 3). (L) Histological score of brain (n = 3). (M) Relative mRNA level of *Zo-1*, *Claudin-1*, and *Occludin* in the brain. (n = 6). Data are presented as ± S.D. *p < 0.05, **p < 0.01, ***p < 0.001.

ischemic stroke and undermines the integrity of the blood-brain barrier [7,8]. Therefore, ferroptosis is a crucial detrimental process in ischemic stroke. A clinical study found that ferritin levels in the plasma and cerebrospinal fluid of patients increased within 24 h after ischemic stroke, and this elevation was associated with early neurological deterioration [9]. The heightened incidence and unfavorable prognosis of ischemic stroke in elderly individuals may also be linked to iron deposition in their brains [10]. In a study of ischemic stroke mice, researchers discovered that liproxstatin-1, an inhibitor of ferroptosis, enhanced the levels of GPX4 and COX2 and facilitated the recovery of neurological functions [11]. Importantly, the initiation of ferroptosis is primarily driven by dysfunctions within the intracellular antioxidant system. The Aryl Hydrocarbon Receptor (AhR) is a nuclear receptor capable of sensing exogenous compounds and certain endogenous molecules, and it indirectly inhibits ferroptosis by upregulating SLC7A11 and thus reduces lipid peroxidation [12,13]. Moreover, AhR activation can synergize with the nuclear transcription factor (Nrf2) to enhance the expression of intestinal tight junction proteins and reduce inflammatory bowel disease [14]. These findings collectively suggest that AhR is a key regulator of both central nervous and intestinal homeostasis and that targeting AhR to suppress ferroptosis may offer a promising therapeutic strategy for ischemic stroke.

Clinically, more than 50 % of patients with ischemic stroke present complex gastrointestinal complications, including dysbiosis of the gut microbiota, dysphagia, constipation, and increased intestinal permeability [15,16]. A clinical cohort study has demonstrated that acute ischemic stroke patients have significant dysbiosis of the gut microbiota, characterized by an overgrowth of *Enterobacteriaceae*, which subsequently exacerbates cerebral infarction [17]. Such evidence has revealed that an interaction exists between the enteric nervous system and the central nervous system, which is referred to as the "gut-brain axis." The central nervous system modulates gut motility, secretion, and microbial composition via neurotransmitters and endocrine signals. In turn, the gut microbiota affects brain function and behavior through neural pathways, immune modulation, and the production of microbial metabolites [18]. Thus, the gut microbiota serves as a critical mediator in the regulation of the gut-brain axis. A study encompassing clinical trials, mouse model experiments, and cell analyses demonstrated that *Blautia producta* causally suppresses microglia-mediated neuroinflammation by regulating the butyrate-RAS-NF-κB axis [19]. Therefore, regulation of the gut microbiome and its metabolites via the gut-brain axis might be a reasonable strategy for the treatment of ischemic stroke.

Akkermansia muciniphila (AKK) is an anaerobic gram-negative bacterium with promising probiotic potential in correcting gut microbiota dysbiosis and intestinal barrier dysfunction [20]. AKK activates the NF-κB signaling pathway in intestinal epithelial cells (IECs) to upregulate MUC2, BIRC3, and TNFAIP3 gene expression, enhancing intestinal barrier function and promoting intestinal homeostasis [21]. In addition to its protective effects on the intestines, AKK has shown therapeutic potential in neurological diseases. A study of 198 patients with ischemic stroke examined the composition of their microbiota and found that the abundance of AKK was significantly lower in stroke patients than in healthy controls [22]. Furthermore, the prophylactic administration of AKK was shown to upregulate various anti-inflammatory factors and significantly mitigate ischemic cerebral infarction in a model of Rose Bengal photothrombosis [23]. This indicates that increased AKK abundance might be beneficial for ischemic stroke. In previous studies, we prepared a novel prebiotic *Puerariae lobatae* Radix-resistant starch (PRS) that was shown to alleviate ischemic stroke-induced damage and promote AKK enrichment in the gut microbiota [24]. Considering that prebiotics can enhance the growth or activity of probiotics, a synbiotic containing a combination of these may exert a synergistic effect on host health. A study indicated that a synbiotic combination of *Lactobacillus rhamnosus* GG and polymannuronate can synergistically enhance the integrity of the blood-brain barrier and increase the expression of GDNF to mitigate apoptosis in the striatum of mice with Parkinson's disease [25]. Thus, synbiotic combinations may exhibit synergistic effects in patients with ischemic stroke. In this study, we aimed to elucidate the effects and mechanisms of AKK in ischemic stroke rats and to investigate whether a novel combination of AKK and PRS could provide a synergistic effect, thereby proposing a new strategy for the prevention and treatment of ischemic stroke.

2. Materials and methods

2.1. Culture of Akkermansia muciniphila

Akkermansia muciniphila (AKK, ATCC BAA-835) was cultured for use in this study. AKK was cultivated anaerobically at 37 ˚C in brain heart infusion (BHI) medium supplemented with 0.5 % type II mucin and 0.05 % L-cysteine for 48 h. AKK pellets obtained by centrifugation were resuspended in anaerobic PBS, and the bacterial concentration was determined by measuring the optical density (OD) at 600 nm. The AKK supernatant was collected by filtration through a 0.22 μm membrane filter. Pasteurized AKK was prepared by heating at 70 ˚C for 30 min before gavage.

2.2. Preparation of PLR-RS

The extraction of PLR-RS was performed as previously described [24]. Briefly, PLR was immersed twice in deionized water, followed by heat treatment. The resulting filtrate was then concentrated. After cooling at 4 ˚C for 48 h, proteins were removed using the Sevage method, followed by dialysis against distilled water for 24 h. The dialyzed solution was precipitated using 83 % ethanol (v/v) at 4 ˚C for 8 h. The precipitate was collected by centrifugation at 4000 rpm for 5 min and then lyophilized to obtain PLR-RS.

2.3. Animals and establishment of model

Male Sprague-Dawley (SD) rats (210 ± 20 g) were purchased from the Laboratory Animal Center of Southern Medical University (Guangzhou, China). All animal care and experimental procedures adhered to the Guidelines for the Care and Use of Laboratory Animals. All protocols were approved by the Experimental Animal Ethics Committee of Southern Medical University.

The middle cerebral artery occlusion/reperfusion (MCAO/R) model was established as previously described [26]. Male SD rats were anesthetized with isoflurane, and transient focal cerebral ischemia was induced via middle cerebral artery occlusion. Rats with a Longa neurological deficit score <2, subarachnoid hemorrhage, or mortality were excluded from further experiments. In the sham-operated group, only the cervical arteries were exposed, while all other procedures were identical to those in the MCAO group.

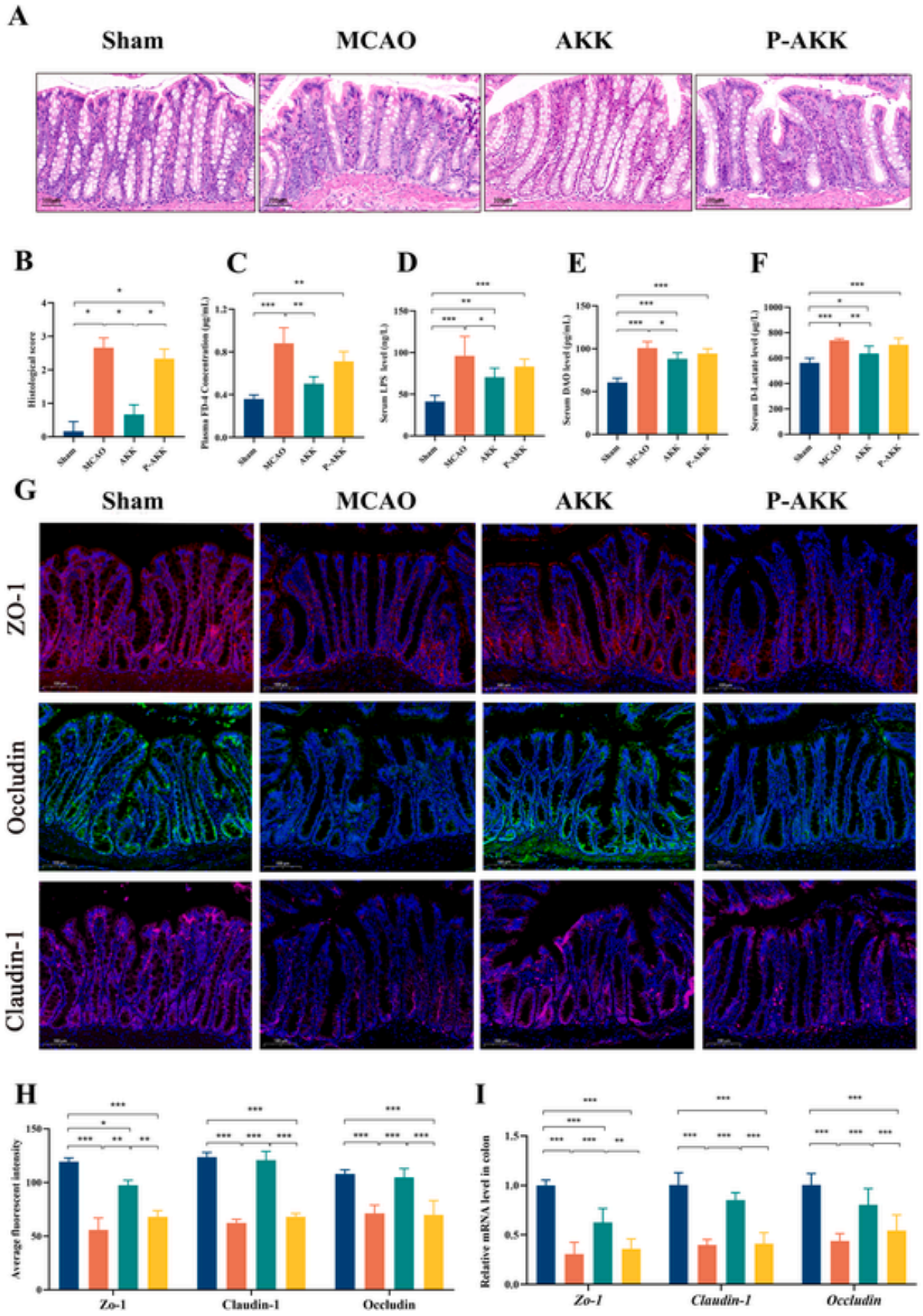
A
Sham
MCAO
AKK
P-AKK
B
Histological score
C
Plasma FD-4 Concentration (μg/mL)
D
Serum LPS level (ng/L)
E
Serum DAO level (pg/mL)
F
Serum D-Lactate level (μg/L)
Sham
MCAO
AKK
P-AKK
G
Sham
MCAO
AKK
P-AKK
ZO-1
Occludin
Claudin-1
H
Average fluorescent intensity
Zo-1
Claudin-1
Occludin
I
Relative mRNA level in colon
Zo-1
Claudin-1
Occludin

Fig. 2. Live AKK attenuated ischemic stroke-induced gut barrier disruption. (A) Representative image of H&E staining in colon (scale bar = 100 μm). (B) The histological score of the colon (n = 3). (C)The concentration of FD-4 in plasma (n = 5). (D–F) The serum levels of LPS, DAO, and D-lactate (n = 6). (G) Immunofluorescence images of tight junction proteins (n = 3), Blue color represents colon cells stained with DAPI, red color represents ZO-1, green color represents Claudin-1, and purple color represents Occludin (Images were taken at × 30 magnification) (H) The average fluorescence intensity densities of ZO-1, Claudin-1 and Occludin (n = 3). (I) Relative mRNA level of *Zo-1 Claudin-1* and *Occludin* in the colon (n = 6). Data are presented as ± S.D. *p < 0.05, **p < 0.01, ***p < 0.001. (For interpretation of the references to color in this figure legend, the reader is referred to the Web version of this article.)

2.4. Animal experiments

To investigate the effects of AKK on ischemic stroke, rats were randomly divided into four groups after a one-week acclimatization period: sham-operated group (Sham), ischemic stroke group (MCAO), live-AKK group (AKK), and pasteurized-AKK group (P-AKK). Rats in the AKK and P-AKK groups received a daily gavage of live or pasteurized AKK (1×10^9 CFU in 200 μL) for 14 days [27]. Meanwhile, the Sham and MCAO groups were gavaged daily with an equal volume of anaerobic PBS. To further investigate the effects of bioactive metabolites produced by AKK on stroke, rats subjected to middle cerebral artery occlusion (MCAO) were randomly divided into two groups: a blank supernatant group (Blank-SUP) and an AKK supernatant group (AKK-SUP). Rats in both groups received a daily oral gavage of 2 mL for 14 days. The supernatant was collected after 48 h of AKK culture, followed by centrifugation and filtration through a 0.22 μm membrane filter [28].

The establishment of a pseudo-germ-free rat model was performed according to previous studies [24]. Rats subjected to middle cerebral artery occlusion (MCAO) were orally administered a mixture of antibiotics (vancomycin 100 mg/kg, neomycin sulfate 200 mg/kg, metronidazole 200 mg/kg, and ampicillin 200 mg/kg) for 4 days to deplete the gut microbiota. After the pseudo-germ-free rat model was established, the animals were randomly divided into two groups: the ischemic stroke group (MCAO-ABX) and the live-AKK group (AKK-ABX). Rats in the AKK-ABX group received live AKK, while those in the MCAO-ABX group were given an equal volume of anaerobic PBS via oral gavage. The intervention was conducted daily for 10 days.

To assess the effect of indole lactic acid on ischemic stroke, rats were divided into three groups: a sham-operated group (Sham), an ischemic stroke group (MCAO), and an indole lactic acid-treated group (ILA). Rats in the ILA group received a daily oral gavage of indole lactic acid (13.84 mg/kg) for 14 days [29]. The other two groups received an equivalent volume of saline.

To validate the roles of AHR and Nrf2 in ILA-mediated ferroptosis inhibition, rats were randomly assigned to four groups: the sham-operated group (Sham), the ischemic stroke group (MCAO), the ILA gavage group (ILA), and the ILA + CH-223191 intervention group (ILA + CH). CH-223191 (Selleck, Houston, USA) was administered at a dose of 5 mg/kg [30]. All interventions were performed once daily for 14 consecutive days.

To investigate the effects of the synbiotic combination on ischemic stroke, rats were randomly assigned to four groups following middle cerebral artery occlusion (MCAO): (1) MCAO group (ischemic stroke model); (2) PRS group, administered 250 mg/kg PRS daily by oral gavage; (3) AKK group, receiving 1×10^9 CFU of live AKK; and (4) synbiotic group, treated with both 250 mg/kg PRS and 1×10^9 CFU of AKK (PRS + AKK) [27]. All interventions were performed once daily for 14 days.

2.5. Neurologic function score and assessment of cerebral infarction

Two neurological scoring methods were used to assess neurological function in ischemic stroke rats: the Longa score and the modified Neurological Severity Score (mNSS) [26]. The Longa score was the classical neurological assessment, while the mNSS was used to evaluate motor, sensory, balance, and reflex functions before MCAO surgery and on days 1, 3, 7, and 14 after treatment. Specific scoring rules are shown in Table S1 and Table S2.

Brain infarction was assessed using TTC staining. Brain sections were incubated in 2 % TTC solution at 37 °C in the dark for 20 min. Slices were then fixed with 4 % PFA and arranged on a black background for imaging and scanning. Infarct areas were analyzed using ImageJ. To eliminate the influence of cerebral edema, the following correction formula was applied: Brain infarction volume (%) = (contralateral volume − non-infarcted ipsilateral volume)/contralateral volume × 100 % [31].

2.6. Nissl staining and haematoxylin-eosin (HE)

Brain and colon tissues were fixed with 4 % paraformaldehyde, embedded in paraffin, and sectioned into 5 μM thick slices, which were mounted on slides. Brain tissues were stained with Nissl or H&E according to standard protocols, while colon tissues were stained with H&E. Pathological scores for brain and colon tissues were referenced from Table S3 and Table S4.

2.7. Immunofluorescence staining

Colon tissues were fixed in 4 % PFA and dehydrated through a graded ethanol series. After permeabilization with PBS, tissues were washed with immunostaining buffer and blocked for 1 h. They were then incubated with the primary antibody at 4 °C overnight, followed by nuclear staining with DAPI. Images were captured using a fluorescence microscope (Eclipse Ti-E, Nikon, Japan).

2.8. Transmission electron microscopy (TEM)

Rat cerebral cortex tissue (1 mm^3) was fixed in 2.5 % formaldehyde solution (G9-16005-500 ML, MACKLIN, USA). After 8 h of fixation at 4 °C, the tissue was dehydrated, embedded, sectioned into ultrathin slices, and stained. Neuronal ultrastructure was then observed under an electron microscope. Samples were imaged on a 200-mesh copper grid (HT7-800/HT7-700, Hitachi, Japan).

2.9. Biochemical analysis

Serum levels of T-CHO, TG, LDL, and HDL were measured using commercial kits (Nanjing Institute of Biotechnology, China) according to the manufacturer's instructions. Brain levels of MDA, SOD, and GSH were also assessed. Serum S100B and GFAP concentrations were determined using ELISA kits (Jiangsu Meimian Industrial Co., Ltd, China).

2.10. Intestinal permeability assay

Rats were orally administered FD-4 at a dose of 200 mg/kg. Four hours later, plasma was collected and used to measure FD-4 levels with a multimode microplate reader (Tecan, Switzerland; excitation/emission = 485/530 nm) [32].

2.11. Metabolomics analysis

Untargeted metabolomics profiling was performed by MetaboProfile (Shanghai, China). The supernatant of the culture was thawed under an ice bath, and the metabolites were extracted at low temperatures after adding acetonitrile containing internal standards. Metabolite analysis was performed by using ultra-performance liquid chromatog-

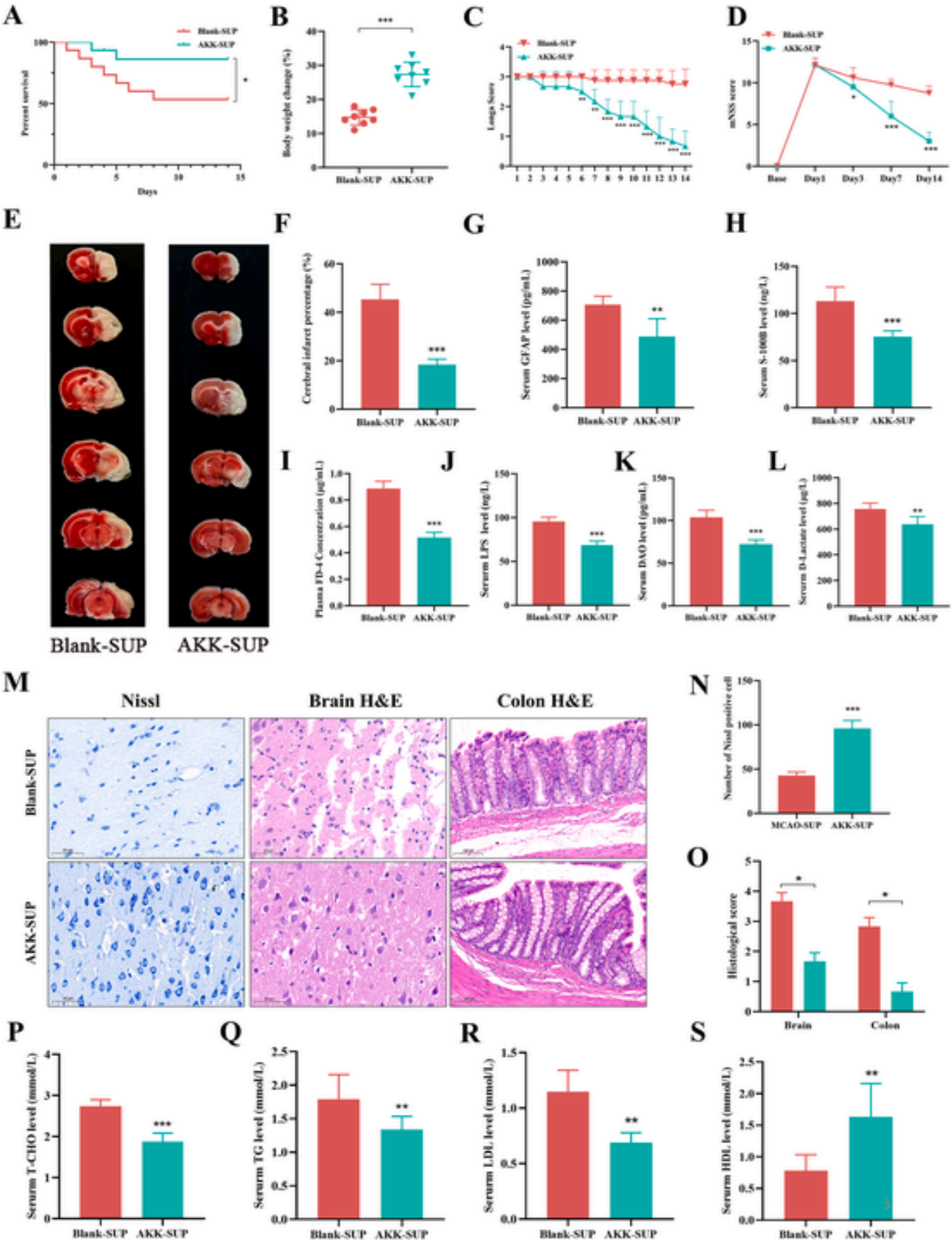
A
Blank-SUP
AKK-SUP
Percent survival
Days
B
Body weight change (%)
Blank-SUP AKK-SUP
C
Longa Score
D
mNSS score
Base Day1 Day3 Day7 Day14
E
Blank-SUP AKK-SUP
F
Cerebral infarct percentage (%)
G
Serum GFAP level (pg/mL)
H
Serum S-100B level (ng/L)
I
Plasma FD-4 Concentration (μg/mL)
J
Serum LPS level (ng/L)
K
Serum DAO level (pg/mL)
L
Serum D-Lactate level (μg/L)
M
Nissl
Brain H&E
Colon H&E
N
Number of Nissl positive cell
MCAO-SUP AKK-SUP
O
Histological score
Brain Colon
P
Serum T-CHO level (mmol/L)
Q
Serum TG level (mmol/L)
R
Serum LDL level (mmol/L)
S
Serum HDL level (mmol/L)

Fig. 3. AKK supernatant mitigates ischemic stroke injury in rats. (A) Survival curve (n = 15). (B)Relative body weight gain for 14 days. (C)Longa score. (D)mNSS score (B-D n = 8). (E)Representative images of TTC staining (n = 4). (F)Quantitative analysis of cerebral infarct areas (n = 4–5). (G–H) Serum level of GFAP and S100B(n = 6). (I)The concentration of FD-4 in plasma (n = 5). (J–L) The serum levels of LPS, DAO, and D-lactate (n = 6). (M) Representative image of Nissl (scale bar = 50 μm), HE (scale bar = 50 μm, 100 μm) staining in brain and colon tissues (n = 3). (N) Quantification of the Nissl staining (n = 3). (O) The Histological scoring of the brain and colon (n = 3). (P–S) Blood lipid in serum: T-CHO, TG, LDL, and HDL (n = 6). Data are presented as ± S.D. *p < 0.05, **p < 0.01, ***p < 0.001.

raphy coupled to a tandem mass spectrometry (UPLCeMS/MS) system (ACQUITY UPLC-Xevo TQ-S, Waters Corp., Milford, MA, USA). The raw UPLCeMS/MS data were processed using the TMBQ software (v1.0, Metabo-Profile, Shanghai, China) to do peak integration, calibration, and quantification for each metabolite. Thereafter, principal component analysis (PCA) was performed by using the self-developed platform iMAP (v1.0, MetaboProfile, Shanghai, China). Statistical analysis and pathway analysis were handled using MetaboAnalyst 5.0.

Indole lactic acid was detected by UPLC-MS/MS. Mobile phase A = 0.1 % formic acid in water; Mobile phase B = 0.1 % formic acid in acetonitrile. The gradient elution process is based on a previous study [28]. Data were processed by MassLynx software (v4.1, Waters, Milford, MA, USA).

2.12. Quantitative real-time PCR (RT-qPCR)

Total RNA was extracted from brain and colon tissue using the Animal Total RNA Isolation Extraction and Purification Kits following the manufacturer's instructions. mRNA was reverse-transcribed into cDNA with the HiScript III All-in-one RT SuperMix and real-time PCR analyses were conducted using the LightCycler 480 and HiScript II Q RT SuperMix. β-actin was used as a control gene. Fecal DNA was extracted using the Tiangen stool DNA extraction kit as per the manufacturer's instructions. 16s was used as a control gene. Relative quantification was calculated by the comparative $2^{-\Delta\Delta CT}$ method. The primer information is listed in Table S5.

2.13. Western blotting assay

The brain tissue was lysed in RIPA buffer containing 1 % cocktail protease inhibitor. The brain proteins were separated by 10 % SDS-PAGE and transferred to a polyvinylidene difluoride (PVDF) membrane. After being blocked with 5 % non-fat milk for 1 h, the membranes were incubated with various primary antibodies overnight at 4 °C, followed by incubation with horseradish peroxidase-conjugated secondary antibody for 1 h at room temperature. The membranes were scanned by a gel image processing system. β-actin was used as the control. The band intensity was assessed using ImageJ software. The antibodies are listed in Table S6.

2.14. In vitro anaerobic culturing and growth curves

For in vitro anaerobic culture experiments, feces from MCAO group rats were collected and processed as previously described [33]. Fecal samples (1.0 g) were resuspended in 10 mL of sterile anaerobic PBS and centrifuged at 5000 × *g* for 1 min at 4 °C to remove impurities. The pellet was washed with 10 mL of sterile anaerobic PBS and centrifuged again at 8000 × *g* for 10 min at 4 °C. The resulting bacterial suspension was resuspended in an acclimatization medium at a ratio of 1:9 (v/v) and incubated under anaerobic conditions at 37 °C for 16 h to activate the bacteria. The fecal inoculum (1:9, v/v) was then transferred to culture media containing either 5 g/L of PLR-RS, inulin, or β-glucan, and incubated anaerobically at 37 °C. Samples were collected at 0, 24, and 48 h, centrifuged at 8000 × *g* for 10 min at 4 °C, and the resulting pellets were collected for DNA extraction and further analysis.

2.15. Statistical analysis

Data were analyzed using IBM SPSS Statistics 25.0 and visualized using GraphPad Prism version 8.0. Results are expressed as mean ± standard deviation (SD). Neurological scores were evaluated using the Kruskal-Wallis test. Significant differences between the two groups were assessed using a two-tailed unpaired Student's t-test, while comparisons among more than two groups were conducted using one-way or two-way ANOVA followed by Tukey's multiple comparisons test. Statistical significance was defined as *P < 0.05, **P < 0.01, and ***P < 0.001. Variable importance in projection (VIP) scores generated by OPLS-DA greater than 1 were considered statistically significant.

3. Results

3.1. Live AKK gavage ameliorates brain injury in rats with ischemic stroke

To investigate the effects of AKK on ischemic stroke, we performed middle cerebral artery occlusion (MCAO) surgery on rats and administered a 14-day gavage of sterile PBS, live AKK, or pasteurized AKK. The results showed that sham-operated rats exhibited no mortality. However, the survival rate was significantly higher in live AKK-treated rats compared to those treated with PBS or pasteurized AKK following ischemic stroke (Fig. 1A: 100 % in the sham group, 50.00 % in the PBS-treated group, 78.50 % in the live AKK-treated group, and 57.33 % in the pasteurized AKK-treated group). Furthermore, compared to the sham group, the MCAO group exhibited a significant reduction in body weight. Live AKK intervention effectively alleviated stroke-induced weight loss, whereas pasteurized AKK failed to produce a similar effect (Fig. 1B). To further assess neurological recovery, we evaluated the Longa score and modified neurological severity score (mNSS). Throughout the observation period, rats in the MCAO group maintained a Longa score of 3 (Fig. 1C), while their mNSS scores remained consistently above 8 (Fig. 1D), indicating that stroke-induced neurological dysfunction does not spontaneously recover over time. In contrast, both assessments consistently demonstrated that live AKK intervention gradually improved neurological function, with significant improvements observed on day 14. Pasteurized AKK, however, failed to alleviate neurological impairment (Fig. 1C and D). Next, we assessed the extent of neurological injury and blood-brain barrier function by measuring serum levels of GFAP and S-100B. According to ELISA results, serum levels of S100B and GFAP were significantly higher in the MCAO group than in the sham group but were significantly reduced following live AKK intervention. No significant differences were observed between the P-AKK and MCAO groups (Fig. 1E and F). Additionally, TTC staining on day 14 after ischemia-reperfusion revealed prominent white infarction and structural collapse in the MCAO group, with an infarction rate of 46.21 %. In contrast, live AKK administration markedly reduced infarct size, lowering the infarction rate to 26.21 %. Pasteurized AKK had no significant effect, with the infarction rate remaining at 40.42 % (Fig. 1G–J). Intriguingly, AKK was successfully colonized in ischemic stroke rats (Fig. S1) and negatively correlated with brain injury markers S100B, GFAP, and cerebral infarction area (Fig. S2). Furthermore, Nissl staining revealed severe neuronal damage in MCAO rats compared to the sham group, including reduction, disintegration, or complete loss of Nissl bodies in the ischemic penumbra. This damage was restored following live AKK treatment (Fig. 1H and K). H&E staining further

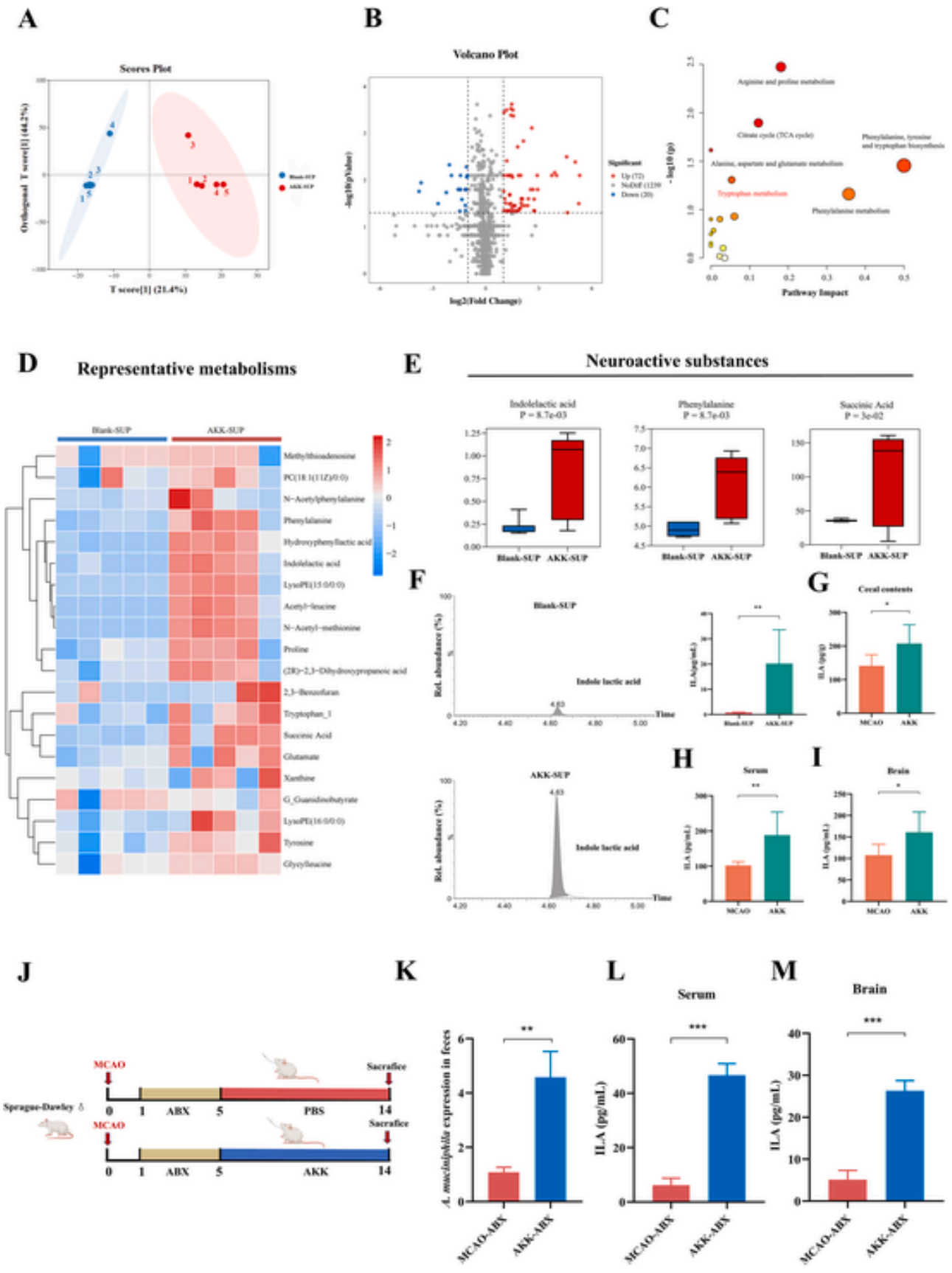
A
Scores Plot
Orthogonal T score[1] (44.2%)
T score[1] (21.4%)
Blank-SUP
AKK-SUP
B
Volcano Plot
-log10(pValue)
log2(Fold Change)
Significant
Up (72)
NoDiff (1239
Down (20)
C
Arginine and proline metabolism
Citrate cycle (TCA cycle)
Phenylalanine, tyrosine and tryptophan biosynthesis
Alanine, aspartate and glutamate metabolism
Tryptophan metabolism
Phenylalanine metabolism
-log10 (p)
Pathway Impact
D
Representative metabolisms
Blank-SUP
AKK-SUP
Methylthioadenosine
PC(18:1(11Z)/0:0)
N-Acetylphenylalanine
Phenylalanine
Hydroxyphenyllactic acid
Indolelactic acid
LysoPE(15:0/0:0)
Acetyl-leucine
N-Acetyl-methionine
Proline
(2R)-2,3-Dihydroxypropanoic acid
2,3-Benzofuran
Tryptophan_1
Succinic Acid
Glutamate
Xanthine
G_Guanidinobutyrate
LysoPE(16:0/0:0)
Tyrosine
Glycylleucine
E
Neuroactive substances
Indolelactic acid
P = 8.7e-03
Phenylalanine
P = 8.7e-03
Succinic Acid
P = 3e-02
Blank-SUP
AKK-SUP
F
Blank-SUP
Indole lactic acid
RoL abundance (%)
Time
AKK-SUP
Indole lactic acid
ILA(ng/mL)
G
Cecal contents
ILA (pg/g)
MCAO
AKK
H
Serum
ILA (pg/mL)
I
Brain
ILA (pg/mL)
J
Sprague-Dawley ♂
MCAO
Sacrafice
0
1
ABX
5
PBS
14
AKK
K
A. muciniphila expression in feces
MCAO-ABX
AKK-ABX
L
Serum
ILA (pg/mL)
M
Brain
ILA (pg/mL)

Fig. 4. AKK generates the biologically active metabolite indole lactic acid. (A) OPLS-DA of metabolic profiling. (B) Volcano map of significant differential metabolites in AKK supernatant compared with Blank supernatant. Significant differential metabolites were identified based on the fold change criteria ≥2 and p-value ≤0.05. The red and blue dots represent significant differential metabolites. (C) Pathway enrichment analysis of the significantly altered metabolites in the supernatants of AKK and Blank groups. (D) Heatmap of representative metabolites. (E) The peak intensities of neuroactive substances. (F) Representative chromatogram and the levels of ILA in the AKK supernatant (A-F n = 5). (G–I) The level of ILA in the cecal contents, serum, and brain samples was detected by ELISA (n = 6). (J) Experimental protocol for pseudo-sterile rats. (K) Relative abundance of AKK in faces (n = 6). (L–M) The level of ILA in the serum and brain samples detected by ELISA (n = 6). Data are presented as ± S.D. *p < 0.05, **p < 0.01, ***p < 0.001. (For interpretation of the references to color in this figure legend, the reader is referred to the Web version of this article.)

showed that the sham group had a structurally intact cerebral cortex with well-defined cells, whereas the MCAO group exhibited a disorganized cortex, cellular necrosis, and liquefaction. Live AKK administration promoted cortical recovery with preserved cell morphology, while pasteurized AKK failed to improve these pathological changes (Fig. 1I and L). We further examined the expression of *Zo-1*, *Occludin*, and *Claudin-1* genes in the brain. Compared with the sham group, the level of tight junction protein was significantly lower in the MCAO group. After live AKK intervention, the level was significantly increased, while pasteurized AKK failed to improve the level of tight junction protein (Fig. 1M). Compared to the MCAO group, the AKK-treated group showed decreased levels of T-CHO, TG, and LDL, and increased HDL levels, suggesting that AKK may improve lipid metabolic disorders and reduce the risk of ischemic stroke (Fig. S3). Taken together, these findings demonstrate that gavage of live AKK, but not pasteurized AKK, ameliorates brain injury in rats with ischemic stroke. This suggests that the protective effects of AKK may depend on bioactive metabolites produced by live bacteria.

3.2. Live-AKK attenuates ischemic stroke-induced gut barrier disruption

Ischemic stroke is often accompanied by intestinal stress, leading to the disruption of intestinal homeostasis, which in turn exacerbates disease progression [34]. Therefore, we next evaluated the effect of AKK on intestinal health in ischemic stroke rats. Histological analysis revealed that rats in the MCAO group exhibited inflammatory cell and lymphocyte infiltration in the lamina propria of the colonic mucosa, accompanied by goblet cell necrosis and widened crypts (Fig. 2A and B). These findings indicate that ischemic stroke is associated with intestinal injury, whereas oral administration of live AKK restored colonic mucosal integrity and alleviated colonic inflammation. In contrast, pasteurized AKK failed to mitigate colonic damage (Fig. 2A and B). Moreover, we assessed markers of intestinal permeability and bacterial translocation, including FD-4, LPS, DAO, and D-lactate. Compared with the sham group, plasma FD-4 and serum levels of LPS, DAO, and D-lactate were significantly elevated in the MCAO group. However, live AKK treatment significantly reduced these indicators, while pasteurized AKK showed no such effect (Fig. 2C–F). These results suggest that intestinal permeability and bacterial translocation are elevated in ischemic stroke rats, and that these abnormalities can be improved through supplementation with live, but not pasteurized, AKK.

Next, we used immunofluorescence to visualize the distribution of tight junction proteins and quantified their expression via fluorescence intensity. In the MCAO group, fluorescence intensity of ZO-1, Occludin, and Claudin-1 was significantly reduced compared to the sham group (Fig. 2G and H), confirming tight junction disruption. Live AKK intervention significantly upregulated the expression of these proteins, especially Occludin and Claudin-1, whose levels approached those of the sham group. In contrast, pasteurized AKK did not improve tight junction protein expression (Fig. 2G and H). Consistent with protein-level findings, gene expression analysis in colonic tissues showed that live AKK upregulated the mRNA levels of *Zo-1*, *Occludin*, and *Claudin-1* (Fig. 2I). The enteric nervous system and the central nervous system interact closely, and positive modulation of this gutbrain axis may contribute to improved disease outcomes. To explore this relationship, we analyzed the correlation of Zo-1, Occludin, and Claudin-1 gene expression between the colon and brain. Interestingly, expression patterns of these tight junction genes were significantly and positively correlated across the two tissues (Fig. S4). In summary, ischemic stroke disrupted the intestinal barrier, as evidenced by structural damage, increased permeability, and reduced tight junction protein expression. Supplementation with live AKK significantly ameliorated these abnormalities, while pasteurized AKK failed to confer protective effects on intestinal injury.

3.3. AKK supernatant mitigates ischemic stroke injury in rats

To investigate the effects of bioactive substances generated by AKK on ischemic stroke, we evaluated whether the culture supernatant from live AKK alleviates brain and intestinal damage in ischemic stroke rats. As anticipated, continuous gavage administration of AKK supernatant for 14 days significantly enhanced the survival rate in ischemic stroke rats and facilitated the restoration of body weight compared with the Blank-SUP group (Fig. 3A and B). In addition, the Longa and mNSS neurological function scores demonstrated that AKK supernatant intervention significantly reduced neurological impairment, suggesting that the AKK supernatant mitigates neurological damage in ischemic stroke models over time (Fig. 3C and D). TTC staining clearly showed that AKK supernatant alleviated cerebral edema and brain collapse in ischemic stroke rats, significantly reducing cerebral infarction volume (Fig. 3E and F). The serum levels of astrocyte markers GFAP and S100B in the AKK-SUP group were significantly lower than those in the Blank-SUP group, indicating that AKK supernatant has the potential to restore blood-brain barrier integrity (Fig. 3G and H). Next, we investigated the effects of AKK supernatant on intestinal injury. The analysis of FD-4 showed that the fluorescence intensity in the serum of ischemic stroke rats treated with AKK supernatant was significantly reduced, implying that intestinal barrier function was improved, leading to a decrease in intestinal permeability (Fig. 3I). Additionally, the levels of serum LPS, DAO, and D-lactate in the AKK-SUP group decreased, further substantiating the recovery of the intestinal barrier (Fig. 3J–L). Nissl and H&E staining of brain tissue showed more Nissl-positive cells and less tissue necrosis and edema in the AKK-SUP group, compared to the Blank-SUP group (Fig. 3M-O). Pathological staining of the colon showed that AKK supernatant intervention reduced the inflammatory response and significantly alleviated pathological phenomena such as epithelial cell shedding and goblet cell loss, compared to pasteurized AKK intervention (Fig. 3M and O). Additionally, AKK supernatant ameliorated lipid profiles and reduced the risk of thrombosis (Fig. 3P–S). These data indicate that live AKK and its culture supernatant protect against neurological dysfunction and intestinal barrier damage in ischemic stroke rats, which may be mediated by the production of biologically active substances.

3.4. AKK generates the biologically active metabolite indole lactic acid

To further investigate the protective substances secreted by AKK, we conducted non-targeted metabolomic analyses on the culture supernatants from blank medium and live AKK medium. Orthogonal partial least squares-discriminant analysis (OPLS-DA) revealed that the metabolite profile of AKK differed significantly from that of the blank medium supernatant (Fig. 4A). We set the screening criteria for differential metabolites as fold change ≥2 and p ≤ 0.05. A total of 72 differ-

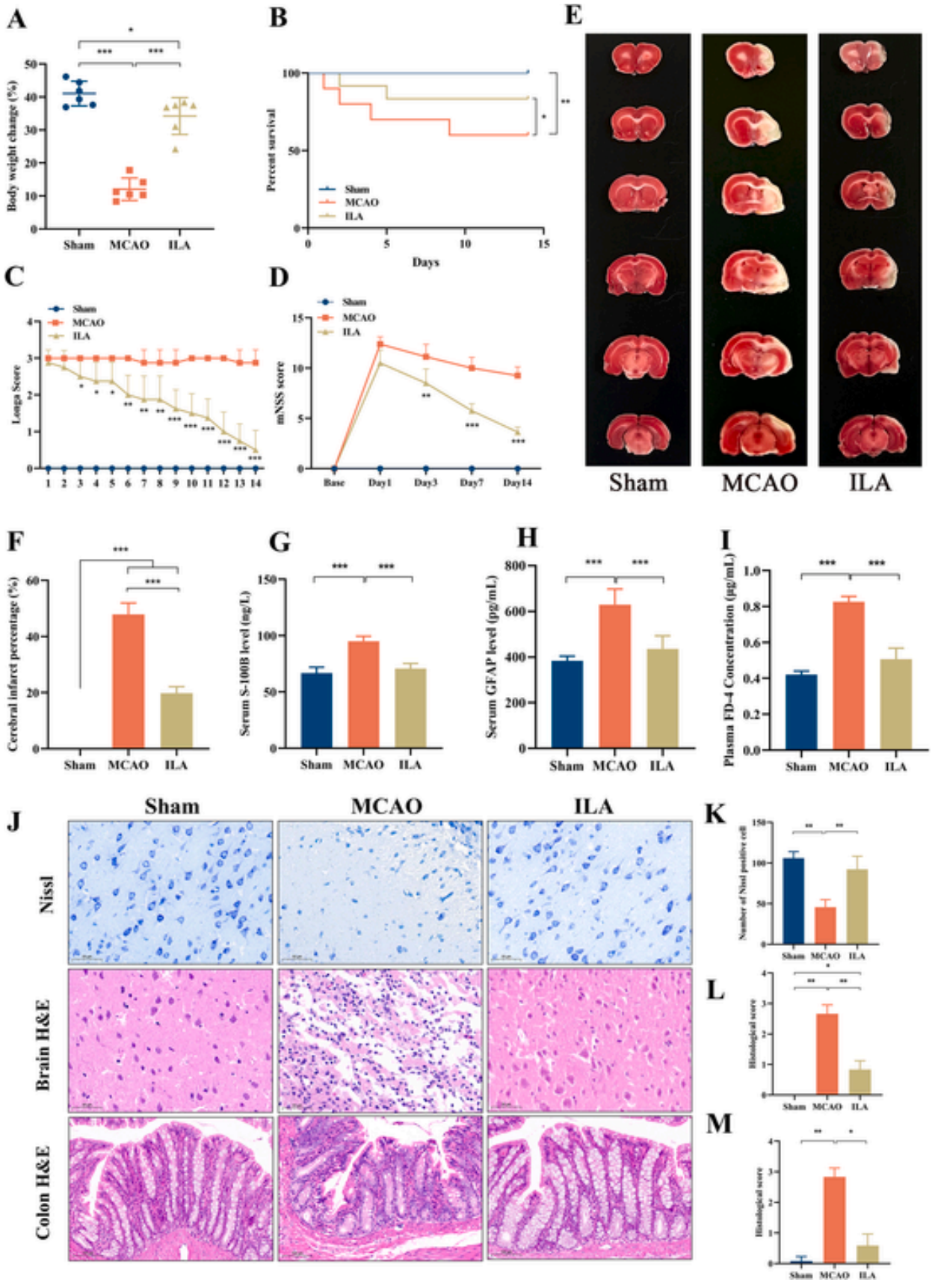
A
Body weight change (%)
Sham
MCAO
ILA
B
Percent survival
Days
C
Longa Score
D
mNSS score
Base
Day1
Day3
Day7
Day14
E
F
Cerebral infarct percentage (%)
G
Serum S-100B level (ng/L)
H
Serum GFAP level (pg/mL)
I
Plasma FD-4 Concentration (μg/mL)
J
Nissl
Brain H&E
Colon H&E
K
Number of Nissl positive cell
L
Histological score
M
Histological score

Fig. 5. Exogenous gavage ILA recapitulates the protective effect of Live-AKK in ischemic stroke rats. (A) Relative body weight gain for 14 days (n = 6). (B) Survival curve (n = 15). (C) Longa score (n = 6). (D) mNSS score (n = 6). (E) Representative images of TTC staining (n = 4). (F) Quantitative analysis of cerebral infarct areas (n = 4). (G–H) Serum level of GFAP and S100B(n = 6). (I)The concentration of FD-4 in plasma (n = 4). (J) Representative image of Nissl (scale bar = 50 μm), HE (scale bar = 50 μm, 100 μm) staining in brain and colon tissues. (K) Quantification of the Nissl staining (n = 3). (L–M) Histological score of brain and colon (n = 3). Data are presented as ± S.D. *p < 0.05, **p < 0.01, ***p < 0.001.

ential metabolites were significantly upregulated in the AKK culture supernatant (Fig. 4B). Based on the KEGG database, these metabolites were classified into functional categories, and five significantly enriched KEGG pathways were identified (Fig. 4C–Table S7). These pathways included the biosynthesis of phenylalanine, tyrosine, and tryptophan; the citrate cycle (TCA cycle); arginine and proline metabolism; alanine, aspartate, and glutamate metabolism; and tryptophan metabolism (Fig. 4C). Heatmap analysis revealed the top 20 metabolites that showed significant changes (Fig. 4D). To identify specific active metabolites related to ischemic stroke, we assessed the potential relevance of each differential metabolite. Several neuroactive substances—such as L-phenylalanine, succinic acid, and indole lactic acid—were significantly upregulated in the AKK supernatant (Fig. 4E).

Indole lactic acid (ILA), a tryptophan-derived metabolite, enhances intestinal barrier function by activating the aryl hydrocarbon receptor (AhR), thereby alleviating intestinal diseases [35]. Therefore, we selected ILA for further investigation in this study to determine whether it is generated by AKK and contributes to its protective effects. To confirm that ILA is produced by AKK, we performed targeted metabolomics on the AKK culture supernatant. We found that ILA levels were significantly higher in the AKK supernatant than in the blank medium supernatant (Fig. 4F), indicating that AKK can produce ILA in vitro. Further validation was conducted in vivo, where we used ELISA to quantify ILA concentrations in the cecal contents, serum, and brain tissue of rats after gavage with live AKK. Our results showed significantly elevated ILA levels in both the cecal contents and peripheral circulation of the AKK group compared to the MCAO group (Fig. 4G–I). To assess the functional role of live AKK in ILA production, we depleted the gut microbiota by administering an antibiotic cocktail, followed by continuous gavage with either live AKK or PBS (Fig. 4J). Our data indicated that AKK was still able to successfully colonize the gut of rats after microbiota clearance (Fig. 4K). Moreover, compared with the MCAO-ABX group, rats colonized with live AKK showed significantly increased ILA levels in both serum and brain tissues (Fig. 4L and M). In conclusion, ILA levels increase with higher AKK colonization in rats, suggesting that AKK produces ILA, which may be a key mediator of its protective effects.

3.5. Exogenous gavage ILA recapitulates the protective effect of live AKK in ischemic stroke rats

To further investigate whether ILA serves as the key active component responsible for the protective effects of AKK against ischemic stroke, we administered exogenous ILA supplementation to stroke rats for 14 consecutive days. Compared with the MCAO group, the survival rate of ILA-treated rats was significantly increased, and body weight was restored by day 14 (Fig. 5A and B). Additionally, Longa and mNSS scores decreased over time following ILA intervention, with significant improvement observed from day 3 and a marked reduction by day 14 (Fig. 5C and D). TTC staining showed that rats treated with ILA exhibited fewer infarcted and collapsed brain areas compared to those in the MCAO group (Fig. 5E and F). Concurrently, the serum levels of S100B and GFAP were significantly elevated in the MCAO group compared to the sham group. However, these levels were markedly reduced following ILA treatment (Fig. 5G and H). Furthermore, ILA significantly reduced plasma FD4 levels, showing no significant difference from the sham group (Fig. 5I), indicating that ILA protects against intestinal barrier dysfunction in ischemic stroke rats. Moreover, Nissl and H&E staining demonstrated that after ILA gavage, neuronal morphology returned to normal, the number of neurons increased, and the cerebral cortex appeared well organized (Fig. 5J–L). Colonic H&E staining revealed that ILA treatment improved epithelial integrity and reduced crypt widening (Fig. 5M). In conclusion, ILA mitigates neurological injury and intestinal barrier dysfunction induced by ischemic stroke, suggesting that it is a pivotal factor mediating the protective effects of AKK.

3.6. ILA activates AhR to inhibit ferroptosis in the brains of ischemic stroke rats

To evaluate whether the protective effect of ILA against ischemic brain injury is associated with the inhibition of ferroptosis, we investigated the influence of ILA on ferroptosis in ischemic stroke rats. Ferroptosis is characterized by programmed cell death triggered by lipid peroxidation mediated by ferrous ions. Compared with the sham group, the level of endogenous ferrous ions (Fe^{2+}) in the brain tissue of MCAO rats was significantly elevated, which was restored to normal levels after ILA treatment (Fig. 6A). We next examined the levels of glutathione (GSH), superoxide dismutase (SOD), and malondialdehyde (MDA) in brain tissue. GSH and SOD levels were significantly decreased in the MCAO group compared to the sham group, whereas MDA levels were significantly increased. However, ILA treatment significantly elevated GSH and SOD levels while reducing MDA levels (Fig. 6B–D). These findings indicate that ILA reduces Fe^{2+} accumulation and lipid peroxidation—key hallmarks of ferroptosis—in ischemic stroke. Furthermore, we used transmission electron microscopy to examine mitochondrial morphology in the cerebral cortex. In the MCAO group, mitochondria displayed increased membrane density, reduced volume, outer membrane rupture, and a significant decrease or complete loss of cristae compared to the sham group. In contrast, ILA-treated rats showed well-defined mitochondrial structures with oval shapes and cristae resembling the normal configuration (Fig. 6E). These data suggest that the neuroprotective effects of ILA during ischemic stroke are closely associated with the inhibition of ferroptosis.

To further explore the mechanism by which ILA alleviates ischemic brain injury, we examined the expression of AhR and Nrf2 in brain tissue. Compared to the sham group, the mRNA levels of AhR and Nrf2 in the MCAO group were significantly decreased, but were markedly elevated following ILA supplementation (Fig. 6F and G). Nrf2 protects brain tissue by activating antioxidant genes that inhibit lipid peroxidation during ferroptosis, thereby reducing oxidative stress and ferroptosis itself. We next assessed the expression of ferroptosis-related genes. The mRNA expression of *Slc7a11* and *Gpx4* was significantly downregulated in MCAO rats compared to the sham group. However, ILA treatment significantly restored their expression (Fig. 6H and I). Interestingly, the levels of brain injury markers (GFAP and S100B) showed significant negative correlations with *AhR*, *Nrf2*, and the ferroptosis-related genes *Slc7a11* and *Gpx4*, further indicating that ferroptosis in the brain is closely associated with the severity of brain injury in ischemic stroke (Fig. S5). In addition, consistent with the mRNA findings, the protein levels of *AhR*, *Nrf2*, *SLC7A11*, and *GPX4* in brain tissue were significantly reduced in the MCAO group compared to the sham group, but were significantly restored following ILA treatment (Fig. 6J–N). These data suggest that ILA ameliorates brain ferroptosis in ischemic stroke by activating the AhR-Nrf2/SLC7A11/GPX4 signaling pathway.

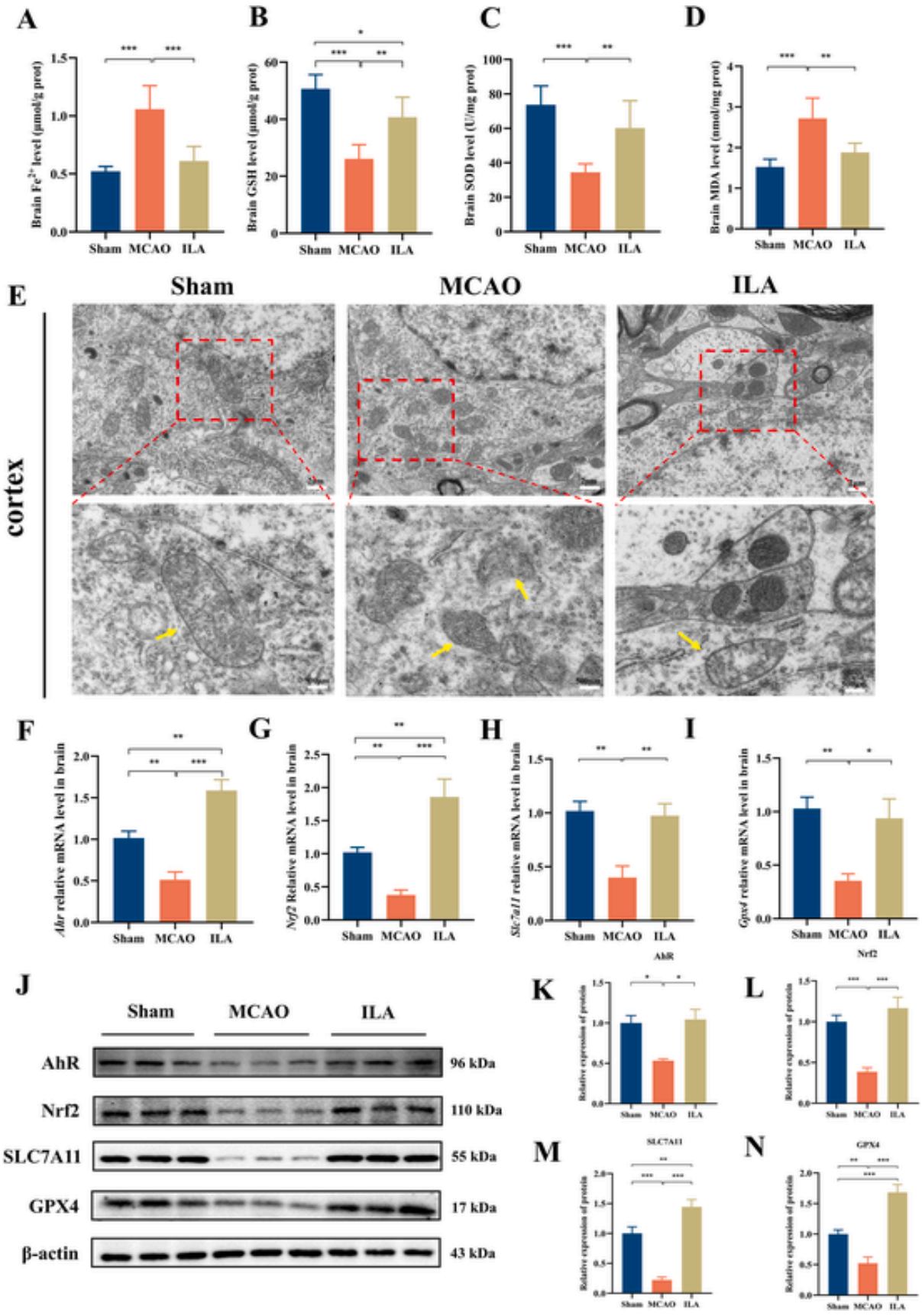
A
Brain Fe2+ level (μmol/g prot)
Sham MCAO ILA
B
Brain GSH level (μmol/g prot)
C
Brain SOD level (U/mg prot)
D
Brain MDA level (nmol/mg prot)
E
Sham
MCAO
ILA
cortex
F
Ahr relative mRNA level in brain
G
Nrf2 Relative mRNA level in brain
H
Slc7a11 relative mRNA level in brain
I
Gpx4 relative mRNA level in brain
J
Sham MCAO ILA
AhR 96 kDa
Nrf2 110 kDa
SLC7A11 55 kDa
GPX4 17 kDa
β-actin 43 kDa
K
AhR
L
Nrf2
M
SLC7A11
N
GPX4
Relative expression of protein

Fig. 6. ILA activates AhR to inhibit ferroptosis in the brains of ischemic stroke rats. (A)The concentrations of Fe^{2+} in the brains of different groups. (B–D) The concentrations of GSH, SOD, and MDA in Brain of different groups. (A-D n = 6). (E) Ultrastructural changes of mitochondria in the cortex by TEM. (F–I) Relative mRNA levels of *Ahr*, *Nrf2*, *Slc7a11,* and *Gpx4* in Brain (n = 6). (J–N) Representative Western blot bands and the relative density analysis results of AhR, Nrf2, Slc7a11, and GPX4 in the Brain. β-actin was set as a loading control (n = 3). Data are presented as ± S.D. *p < 0.05, **p < 0.01, ***p < 0.001.

3.7. Inhibition of AhR activation in the brain abolished the protective effects of ILA

To further examine whether the protective effects of ILA against ferroptosis in the brain tissue of ischemic stroke rats are mediated by AhR signaling, we treated ischemic stroke rats with the AhR antagonist CH223191(Fig. 7A). We first evaluated the expression of the AhR in the brain tissue of ischemic stroke rats following inhibitor intervention. The results showed that treatment with CH223191 significantly reduced the AhR mRNA levels in the ILA + CH group (Fig. S5A). Furthermore, the inhibition of AhR led to a decreased expression of Nrf2, as well as ferroptosis-related genes SLC7A11 and GPX4 (Figs. S5B–D). These findings indicate that the CH223191 intervention effectively suppressed AhR signaling.

After confirming the suppression of AhR signaling, we assessed neurological function and brain injury in rats from the ILA + CH223191 group. The results indicated that, compared to the ILA group, the ILA + CH223191 group exhibited reduced recovery in body weight and lower survival rates (Fig. 7B and C). Moreover, both the mNSS and Longa neurological scores consistently showed poorer neurological recovery in ischemic stroke rats following inhibitor treatment, with a significant decline in scores compared to the ILA group (Fig. 7D and E). These findings suggest that AhR inhibition counteracts the beneficial effects of ILA intervention on body weight recovery, survival rate, and neurological function in ischemic stroke rats.

The TTC staining results of brain tissue further revealed no significant difference in cerebral infarction between the ILA + CH223191 group and the MCAO group (Fig. 7F and G). Additionally, compared to the ILA group, serum levels of brain injury markers GFAP and S-100B were elevated in the ILA + CH223191 group, indicating that CH223191 intervention abolished the protective effect of ILA (Fig. 7H and I). Nissl staining showed that the ILA + CH223191 group exhibited blurred and significantly reduced Nissl body profiles (Fig. 7J and K). H&E staining demonstrated that the cerebral cortex structure in the ILA + CH223191 group was disorganized, with loose architecture, fragmentation into numerous small pieces, and cell necrosis, similar to the damage observed in the MCAO group (Fig. 7J and L). Furthermore, compared to the ILA group, the levels of ferrous ions (Fe^{2+}) and lipid peroxides (MDA) were significantly increased, while the levels of glutathione (GSH) and superoxide dismutase (SOD) were significantly decreased in the ILA + CH223191 group (Fig. 7M-P). These findings suggest that inhibition of AhR signaling partially counteracts the protective effect of ILA on ischemic stroke.

3.8. Symbiotic combination of AKK and PRS exhibits a synergistic effect to mitigate ischemic stroke

In our previous research, we developed a novel prebiotic, PRS (*Puerariae Lobatae* Radix-resistant starch), which significantly enriched AKK in vivo and alleviated ischemic stroke injury [24]. To further evaluate the AKK-enriching potential of PRS, we conducted an in vitro experiment. Fresh feces from MCAO rats were anaerobically co-cultured with different prebiotics, including PRS, inulin, and β-glucan (Fig. 8A). After 48 h of co-culture, AKK abundance was significantly increased in samples treated with PRS compared to the control group (microbiota cultured without prebiotics), while neither inulin nor β-glucan promoted AKK enrichment (Fig. 8B). These findings suggest that PRS selectively enriches AKK. To further verify the enrichment capacity of PRS, we collected bacterial pellets from the co-culture system at 0, 24, and 48 h and measured AKK abundance. At 0 h, no significant difference was observed between groups. However, at 24 and 48 h, AKK levels were consistently and significantly higher in the PRS-treated group (Fig. 8C). Additionally, higher concentrations of ILA were detected in the supernatants of PRS co-cultures (Fig. 8D), and ILA levels were positively correlated with AKK abundance (Fig. 8E). These results indicate that PRS selectively enriches AKK and promotes ILA production in vitro. The combination of probiotics and prebiotics has been reported to generate a synergistic effect, conferring more benefits to the host. Therefore, we investigated in vivo whether combining AKK and PRS probiotics could synergistically enhance protection against ischemic stroke injury. Compared with the rats in the MCAO group, the body weight of the PRS, AKK, and synbiotic groups recovered to different extents. Among them, the synbiotic composed of PRS and AKK intervention had the best effect on the body weight recovery of rats with ischemic stroke (Fig. 8F). Survival analysis revealed that AKK alone improved survival, whereas PRS alone did not. Notably, the synbiotic significantly increased the survival rate to 87.5 %, indicating that the combined intervention offers greater protection against stroke-related mortality (Fig. 8G). Neurological assessments using Longa and mNSS scores consistently demonstrated that the synbiotic group exhibited superior neurological recovery compared to PRS or AKK alone (Fig. 8H and I). Similarly, TTC staining showed that the synbiotic more effectively alleviated brain edema and tissue collapse, reducing the infarct volume to 10.37 % (Fig. 8J and K). Serum levels of S100B and GFAP, both of which were elevated in the MCAO group, were significantly reduced by PRS or AKK intervention, and even more so in the synbiotic group (Fig. 8L and M), suggesting an enhanced protective effect on blood–brain barrier integrity. Furthermore, intestinal permeability was reduced in all three treatment groups compared to the MCAO group, with greater reductions observed in the AKK and synbiotic groups than in the PRS group (Fig. 8N). Collectively, these findings suggest that the synbiotic combination of PRS and AKK synergistically alleviates cerebral injury and restores intestinal barrier function in rats with ischemic stroke.

4. Discussion

The pathological process of ischemic stroke can be exacerbated by intestinal barrier disruption caused by gut microbiota dysbiosis [36,37]. Therapeutic modulation of the gut microbiome using probiotics or prebiotics has demonstrated beneficial effects in patients with ischemic stroke [38,39]. In our study, live AKK was proven to generate ILA, which inhibits ferroptosis in the brain by activating AhR and upregulating the expression of Nrf2 to alleviate ischemic stroke-induced damage. Moreover, the abundance of AKK in the intestine was selectively enriched by a novel prebiotic, PRS, which in turn promotes ILA production. Notably, a symbiotic combination of AKK and PRS had a synergistic effect in alleviating ischemic stroke impairment. Thus, our findings confirm the therapeutic effect of AKK and its bioactive product ILA on ischemic stroke and showcase a novel synbiotic therapy that may synergistically alleviate ischemic stroke.

AKK is a gram-negative anaerobic bacterium that accounts for 1 %–5 % of the gut microbiome in healthy individuals and has promising probiotic activities that can fight many diseases [20]. Compared with the intestinal microbiome of the healthy control group, that of patients with ischemic stroke had a significantly decreased abundance of AKK [22]. AKK resides in the intestinal mucosal layer and degrades mucins using fucosidases and sialidases to obtain the sole source of carbon and nitrogen required for its growth [40–42]. Upon mucin degradation, AKK releases metabolites including monosaccharides, oligosaccharides, and short-chain fatty acids. These compounds serve as nutri-

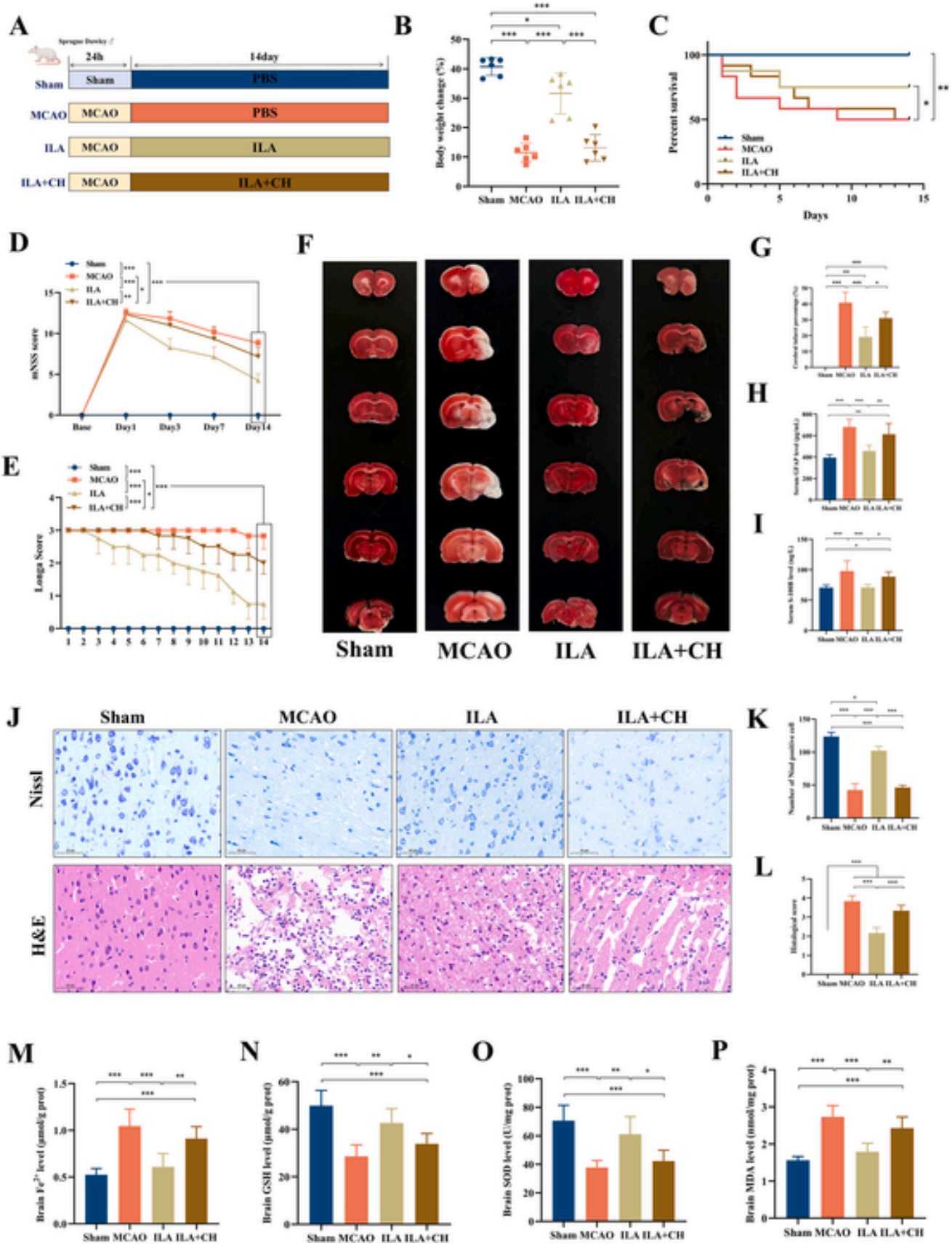
A
24h
14day
Sham
PBS
MCAO
PBS
ILA
ILA
ILA+CH
ILA+CH
B
Body weight change (%)
Sham MCAO ILA ILA+CH
C
Percent survival
Days
Sham
MCAO
ILA
ILA+CH
D
mNSS score
Base Day1 Day3 Day7 Day14
E
Longa Score
F
Sham
MCAO
ILA
ILA+CH
G
H
I
J
Sham
MCAO
ILA
ILA+CH
Nissl
H&E
K
L
M
Brain Fe2+ level (μmol/g prot)
N
Brain GSH level (μmol/g prot)
O
Brain SOD level (U/mg prot)
P
Brain MDA level (nmol/mg prot)

Fig. 7. Inhibition of brain AhR activation abolished the protective effects of ILA. (A)Experimental design diagram (B) Relative body weight gain for 14 days (n = 6). (C) Survival curve (n = 15). (D) mNSS score (n = 6). (E) Longa score (n = 6). (F) Representative images of TTC staining (n = 4). (G) Quantitative analysis of cerebral infarct areas (n = 4). (H–I) Serum level of GFAP and S100B(n = 6). (J) Representative image of Nissl (scale bar = 50 μm), HE (scale bar = 50 μm, 100 μm) staining in brain tissues. (K) Quantification of the Nissl staining (n = 3). (L) Histological score of brain (n = 3). (M)The concentrations of Fe^{2+} in the brains of different groups. (N–P) The concentrations of GSH, SOD, and MDA in Brain of different groups. Data are presented as ± S.D. *p < 0.05, **p < 0.01, ***p < 0.001.

ents for other microbes and help maintain intestinal microbial homeostasis. At the same time, AKK promotes the generation of mucus via feedback regulation to maintain the integrity of the gastrointestinal tract [42–44]. A recent study reported that supplementing with AKK can facilitate the growth of *Bifidobacterium* and *Lactobacillus*, counteracting the colonization of pathogenic bacteria within the intestinal tract to mitigate the impairment of inflammatory bowel disease [45,46]. Additionally, AKK and its membrane protein Amuc_1100 were found to ameliorate intestinal inflammatory stress and promote epithelial wound healing via cAMP-responsive element-binding protein H and microRNA-143/145 [47]. Together, these findings support the pivotal role of AKK in regulating intestinal homeostasis and alleviating injury. In the present study, we observed that ischemic stroke led to inflammatory cell and lymphocyte infiltration in the colonic submucosa, accompanied by morphological changes in crypts and goblet cells. These pathological alterations were effectively reversed following AKK intervention. AKK intervention enhanced the expression of intestinal tight junction proteins, particularly Claudin-1 and Occludin, restoring their levels to those observed in healthy controls. Claudin 1 regulates the selective permeability of tight junctions to ensure the controllability of substances within the intercellular space; while occludin supports and modulates the structural stability of tight junctions, helping them withstand environmental stress and influencing their plasticity [48,49]. Therefore, these two proteins synergistically uphold the integrity of the intestinal barrier. Intervention with AKK decreased the intestinal permeability of the rat models and attenuated the entry of DAO, lipopolysaccharides, and D-lactate into the systemic circulation. Thus, our findings suggest that AKK enhanced intestinal barrier function to prevent translocation in the ischemic stroke rats. In addition to alleviating intestinal damage, we observed that the levels of tight junction proteins *Zo-1*, *Claudin-1*, and *Occludin* in the brain were elevated after AKK intervention. It has been reported that the tight junction proteins between cells guarantee the physical function of the blood-brain barrier, including its ability to restrict the transport of harmful substances in the periphery and maintain the stability of the internal environment in the center [48]. We found that the serum concentrations of GFAP and S100B markedly decreased after AKK intervention. As biomarkers of neuroglial cells in the brain, GFAP and S100B are associated with neuronal injury, inflammatory responses, and cell death and are released into the bloodstream after damage to the blood-brain barrier [50]. Hence, our findings indicate that AKK intervention also mitigated the impairment of the blood-brain barrier in ischemic stroke rats. Interestingly, we found a positive correlation between the alterations in tight junction proteins in the brain and colon of ischemic stroke rats after AKK intervention (Fig. S4). This prompted us to speculate that the alleviation of ischemic stroke might have been associated with intestinal barrier repair, which lowered the risk of systemic inflammation and gastrointestinal complications and prevented harmful substances from entering the blood.

In addition, ischemic stroke in rats led to body weight loss and reduced survival rates. This may have been because stroke led to an inadequate energy supply, increasing the metabolic burden, and promoting the catabolism of muscle and adipose tissue. Stroke influenced the appetite and physical activities of the rats, causing a decrease in energy intake and consumption and leading to weight loss [51,52]. This weight loss precipitated malnutrition and immune dysfunction in the animals, increasing their susceptibility to infections while concurrently diminishing their recovery capacity, and thereby significantly impacting survival rate [53]. However, AKK intervention increased the body weight and survival rate of ischemic stroke rats and significantly reduced cerebral infarction volume. We speculated this may have been attributable to AKK's repair of the intestinal damage caused by ischemic stroke, which increased intestinal absorption and the utilization of nutrients and thus led to weight gain. Weight loss is an independent risk factor for mortality in stroke model rats, and the weight gain resulting from AKK intervention improved their recovery ability and enhanced their immunity, leading to a significant improvement in their survival rate. A recent study of a Rose Bengal photothrombotic model confirmed our findings, with the prophylactic administration of AKK significantly upregulating various anti-inflammatory factors and markedly reducing ischemic cerebral infarction [23]. In this study, we employed middle cerebral artery embolization to establish the stroke model, which is more consistent with the pathogenic mechanism of clinical cerebral infarction. Our research findings indicate that therapeutic intervention with AKK significantly mitigates the adverse outcomes occurring in the gut and brain after ischemic stroke, deepening our understanding of its potential mechanisms of action within central nervous system pathologies.

Probiotics influence their host's health through multiple pathways, including direct interaction with host cells, secretion of metabolites, modification of the host microecological balance, and activation of immune responses [54]. Our findings demonstrate that live AKK, but not pasteurized AKK, attenuates ischemic-stroke-induced brain impairment and gut barrier dysfunction. This suggests that AKK's protective effect against ischemic stroke may be mediated by the bioactive metabolites it produces. However, pasteurization disrupts the structure of AKK, rendering it biologically inactive and incapable of performing essential metabolic processes such as enzyme catalysis, material synthesis, and energy conversion, which are necessary for metabolite production. Studies have shown that certain bacterial metabolites can readily cross through the intestinal barrier and enter the bloodstream, reaching pathological sites due to their simple structures and relatively small molecular weights [54–56]. Therefore, identifying and characterizing these active small-molecule metabolites may provide deeper insight into how AKK influences ischemic stroke. In our study, live AKK was shown to generate ILA in vivo and in vitro conditions, which to our knowledge has not previously been reported. ILA, a tryptophan metabolite, has been reported to safeguard intestinal health by enhancing the intestinal barrier via its anti-inflammatory, antioxidant, and immunoregulatory effects. A study has shown that ILA alleviates lipopolysaccharide-induced intestinal barrier damage and HT-29 cell monolayer inflammation by activating AhR and Nrf2 while inhibiting the NF-κB signaling pathway [57]. In addition to its protective effects on the intestines, ILA has been found to improve central nervous system disorders. ILA enhances neurite outgrowth in PC-12 cells and inhibits neurodegeneration in HT-22 cells [58]. These findings suggest that ILA has promising effects on the regulation of the intestine and brain. In our study, the exogenous administration of ILA was confirmed to improve the brain and intestinal damage caused by ischemic stroke. Notably, ILA treatment led to faster neurological recovery and reduced infarct volume compared to AKK treatment. This might have been attributable to the relatively small molecular weight of ILA, which enabled it to rapidly enter the bloodstream, traverse the blood-brain barrier, and alleviate damage at the cerebral infarction site. Therefore, we hypothesize that the reparative effects of AKK on brain and intestinal injury are at least partially mediated by ILA, a bioactive metabolite produced by

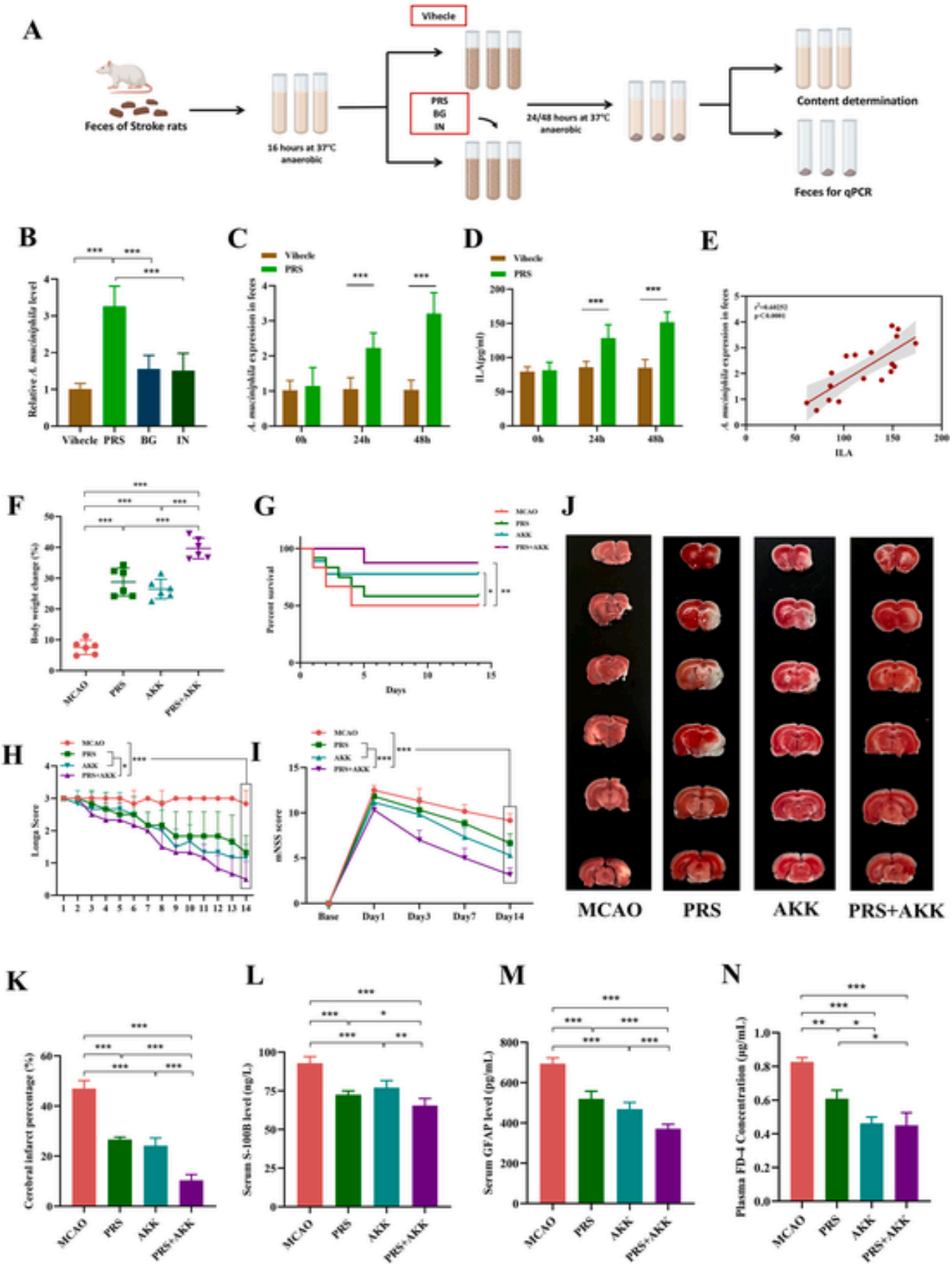
A
Feces of Stroke rats
16 hours at 37°C anaerobic
Vihecle
PRS
BG
IN
24/48 hours at 37°C anaerobic
Content determination
Feces for qPCR
B
Relative A. muciniphila level
Vihecle PRS BG IN
C
Vihecle
PRS
A. muciniphila expression in feces
0h 24h 48h
D
Vihecle
PRS
ILA(pg/ml)
0h 24h 48h
E
A. muciniphila expression in feces
ILA
F
Body weight change (%)
MCAO PRS AKK PRS+AKK
G
MCAO
PRS
AKK
PRS+AKK
Percent survival
Days
H
Longa Score
I
mNSS score
Base Day1 Day3 Day7 Day14
J
MCAO PRS AKK PRS+AKK
K
Cerebral infarct percentage (%)
MCAO PRS AKK PRS+AKK
L
Serum S-100B level (ng/L)
MCAO PRS AKK PRS+AKK
M
Serum GFAP level (pg/mL)
MCAO PRS AKK PRS+AKK
N
Plasma FD-4 Concentration (μg/mL)
MCAO PRS AKK PRS+AKK

Fig. 8. A symbiotic combination of AKK and PRS exhibits a synergistic effect to mitigate brain damage. (A) Schematic of AKK enrichment by PRS in vitro. (B) Relative mRNA levels of AKK in the co-culture system. (C) Relative mRNA levels of AKK in a co-culture system at 0 h, 24 h, and 48 h. (D) The level of ILA in a co-culture system at 0 h, 24 h, and 48 h. (A-D n = 6) (E) The correlation between the abundance of AKK and the level of ILA in the co-culture system. (F) Relative body weight gain for 14 days (n = 6). (G) Survival curve (MCAO group n = 12, PRS group n = 12, AKK group n = 9, PRS group n = 8). (H) Longa score (n = 6) (I) mNSS score (n = 6) (J) Representative images of TTC staining (n = 4) (K) Quantitative analysis of cerebral infarct areas (n = 4–5) (L–M) Serum level of S100B and GFAP (n = 6). (N) The concentration of FD-4 in plasma (n = 5). Data are presented as ± S.D. *p < 0.05, **p < 0.01, ***p < 0.001.

AKK. While our study demonstrated the protective effects of ILA on brain and intestinal injuries in ischemic stroke, the precise mechanism by which live AKK produces ILA remains elusive and requires further investigation. Studies have shown that ILA biosynthesis is closely associated with tryptophan metabolism, with *Lactobacillus* and *Bifidobacterium* converting ingested tryptophan into ILA via tryptophan dehydrogenase [59,60]. Hence, we hypothesized that live AKK may possess structural similarities to tryptophan dehydrogenase, enabling it to facilitate ILA production. Additionally, we cannot rule out the possibility that there are translation-independent pathways that form ILA in live AKK. Thus, future research will focus on uncovering the precise mechanisms underlying ILA production by AKK. In addition to small-molecule metabolites, other active metabolites of AKK have shown potential in protecting host health. Chen et al. revealed that metabolism by AKK generates a novel tripeptide, RKH (Arg-Lys-His), that significantly attenuates the activation of inflammatory cells and the excessive production of pro-inflammatory factors, thereby conferring protective effects against the mortality and organ damage associated with sepsis [28]. Xie et al. found that the AKK metabolite harmaline inhibited systemic inflammation via transmembrane G-protein coupled receptor-5–NF-κB signaling [61]. Thus, other metabolites produced by live AKK may also play regulatory roles in ischemic stroke, and further research is warranted to identify additional key biologically active metabolites.

Although we have confirmed that the ILA generated by AKK can protect against the intestinal and brain damage caused by ischemic stroke, how ILA exerts its protective effects is still unclear. ILA, an endogenous ligand of AhR, has been shown to upregulate Nrf2 expression through the activation of AhR [57,62]. Nrf2 serves as a critical transcription factor in the cellular response to oxidative stress, maintaining homeostasis by regulating the antioxidant defense system and exerting inhibitory effects on ferroptosis [63]. Ferroptosis is an iron-dependent form of cell death characterized by lipid peroxidation and an imbalance of the antioxidant system [12]. The oxidative stress caused by ischemia and reperfusion leads to the excessive generation of ROS, and iron metabolism disorders aggravate the Fenton reaction, further promoting lipid peroxidation and ultimately causing damage to the blood-brain barrier and neurons [64]. In this study, an abnormal elevation of iron concentrations, an accumulation of lipid peroxides, and disordered mitochondrial structures were observed in the brain tissue of rats with ischemic stroke, which confirmed the involvement of ferroptosis in the pathological process. SLC7A11 is responsible for importing the cysteine needed for the synthesis of glutathione and antioxidant defenses against ferroptosis, while GPX4 is an enzyme that participates in cellular antioxidant reactions and removes peroxides to maintain the oxidation-reduction balance within cells [12]. Notably, 14 days after the occurrence of ischemic stroke, the levels of AhR, Nrf2, and ferroptosis-related factors SLC7A11 and GPX4 consistently decreased in the brain tissue of the rats. However, after ILA intervention, the levels of AhR, Nrf2, and ferroptosis-related proteins were upregulated in brain tissue, Fe^{2+} levels were restored to normal, the accumulation of lipid peroxides was reduced, and mitochondrial structures tended to normalize. Importantly, the administration of an AhR inhibitor abolished the protective effects of ILA, indicating that ILA may mitigate brain injury in ischemic stroke rats by inhibiting ferroptosis through AhR activation. However, the use of a single AhR inhibitor in this study was insufficient to fully elucidate the role of AhR. To further validate the significance of AhR in ILA-mediated neuroprotection, future studies should incorporate inhibitors with diverse properties and AhR-knockout rat models.

In the present study, increasing the abundance of AKK in the gut of rats with ischemic stroke and increasing the content of ILA in the systemic circulation were effective strategies for alleviating intestinal and brain damage. Recent studies have shown that the abundances of beneficial bacteria and their metabolites can be promoted through prebiotics, which resist decomposition by digestive enzymes in the gastrointestinal tract and offer fermentable nutrients that allow probiotics to improve the intestinal microecological balance and sustain the host's health [65,66]. Our study investigated the AKK-enrichment capacity of three prebiotics, inulin, β-glucose, and PRS. Inulin is an oligosaccharide composed of fructose units; β-glucan is composed of glucose units connected through β-1,3- and β-1,4-glycosidic bonds; and PRS is composed of two glucose polymers, amylose and amylopectin. Our findings demonstrated that the abundance of AKK in gut microbiome species cultured with inulin and β-glucose remained unchanged, while the abundance of AKK among gut microbiome species cultured with PRS increased, and the increase was significantly positively correlated with the content of ILA in the co-culture supernatant. These findings indicated that PRS can selectively enrich AKK and facilitate the generation of ILA. Although all three prebiotics have been documented to facilitate the growth of probiotics, their distinctive structures give rise to diverse properties. We speculate that AKK possesses a key enzyme structure for degrading and utilizing PRS, providing nutrients for its growth, yet this supposition demands further exploration and verification. Our previous research demonstrated that PRS can alleviate ischemic stroke-related damage in rats by promoting the growth of specific intestinal bacteria (including *Akkermansia* and *Bifidobacterium*). Here, our results further highlight the AKK-enrichment capability of PRS. Synbiotics are defined by the International Scientific Association for Probiotics and Prebiotics as mixtures of live microorganisms and substrates selectively utilized by the host microbiome [67]. Compared to the individual use of probiotics or prebiotics, synbiotics offer a distinct advantage due to their synergistic efficacy [68]. One study found that a synbiotic combination of *Lactobacillus reuteri* and inulin alleviated ASD-like behaviors in a mouse model by reducing the expression of inflammatory cytokines in the brain [69]. In another study, a synbiotic combination containing *Lactobacillus rhamnosus* GG and polymannuronate synergistically enhanced the integrity of the blood–brain barrier and increased the expression of GDNF to mitigate cell apoptosis in the striatum of Parkinson's disease mice [25]. Considering that PRS is capable of enhancing the growth and metabolic activity of AKK, a synbiotic combination of AKK and PRS might exert a synergistic effect in mitigating ischemic stroke injury. Our findings show that using a combination of AKK and PRS as a synbiotic was more effective for improving the weight, survival rate, and recovery of neurological function of ischemic stroke rats than AKK or PRS intervention alone, and it significantly reduced the incidence of cerebral infarction. This indicates that a novel synbiotic combination could be used to optimize the efficacy of ischemic stroke treatments. Although the mechanisms of action of synbiotic combinations are likely to be similar to those of single-strain therapies and prebiotic interventions, their precise modes of action remain inadequately explored. Given the synergistic effects of combined probiotics and prebiotics, as well as their broad impact on the gut microbiota, combination therapies are likely to involve more complex mechanisms. Compared to single-strain therapy, the dynamic interactions within synbiotic formulations may enhance gut homeostasis and amplify therapeutic effects by modulating microbial composition, metabolic pathways, and immune responses. However, further research is needed to elucidate the specific contributions

of individual bacterial strains and their synergistic interactions with prebiotics. This understanding is crucial for optimizing microbiota-based therapeutic strategies and advancing personalized medicine.

5. Conclusion

This study revealed that supplementation with AKK can alleviate ischemic stroke injury, partially due to its production of ILA, which inhibits ferroptosis in the brain. Notably, the combination of AKK and PRS formed a novel synbiotic that exhibited a considerable synergistic effect in alleviating ischemic stroke damage. Our findings provide evidence supporting the potential application of synbiotics as neuroprotective therapies.

CRediT authorship contribution statement

Jiahan Wang: Writing – review & editing, Writing – original draft, Methodology, Investigation. **Yongzheng Peng:** Methodology, Investigation. **Yarui Liu:** Methodology, Data curation. **Zhuoshi Lian:** Validation, Investigation. **Zheng Cai:** Validation, Investigation. **Ye Chen:** Project administration, Formal analysis. **Haoqing He:** Supervision, Conceptualization. **Meilin Yang:** Visualization. **Jie Zhao:** Writing – review & editing, Visualization, Methodology, Investigation.

Ethics statement

No experiments involving human subjects were performed in this study. The animal research was approved by the Animal Experiment Ethics Committee of the Southern Medical University.

Data availability

The main data are contained in the main manuscript and the additional file. Detailed data will be made available upon request.

Funding

This work was supported by the Natural Science Foundation of Guangdong Province (2020A1515011339, 2023A1515012565, 2024A1515010462) and the Science and Technology Project of Shenzhen (KCXFZ20211020163558024).

Declaration of competing interest

The authors declare no conflicts of interest.

Acknowledgement

We thank Metabo-Profile (Shanghai, China) for their excellent technical assistance with metabolomics analysis, and Figdraw (www.figdraw.com) for the preparation of the graphical abstract.

Appendix A. Supplementary data

Supplementary data to this article can be found online at https://doi.org/10.1016/j.freeradbiomed.2025.04.020.

References

[1] S.J. Mendelson, et al., Diagnosis and management of transient ischemic attack and acute ischemic stroke: a review, JAMA 325 (11) (2021) 1088–1098, https://doi.org/10.1001/jama.2020.26867.
[2] V.L. Feigin, et al., Pragmatic solutions to reduce the global burden of stroke: a world stroke organization-lancet neurology commission, Lancet Neurol. 22 (12) (2023) 1160–1206, https://doi.org/10.1016/s1474-4422(23)00277-6.
[3] C.D. Maida, et al., Molecular pathogenesis of ischemic and hemorrhagic strokes: background and therapeutic approaches, Int. J. Mol. Sci. 25 (12) (2024) 6297, https://doi.org/10.3390/ijms25126297.
[4] Ł. Przykaza, Understanding the connection between common stroke comorbidities, their associated inflammation, and the course of the cerebral ischemia/reperfusion cascade, Front. Immunol. 12 (2021) 782569, https://doi.org/10.3389/fimmu.2021.782569.
[5] F. Sun, et al., No-reflow after recanalization in ischemic stroke: from pathomechanisms to therapeutic strategies, J. Cerebr. Blood Flow Metabol. : Off. J. Int. Soc. Cerebr. Blood Flow Metabol. 44 (6) (2024) 857–880, https://doi.org/10.1177/0271678x241237159.
[6] J.X. Ren, et al., Crosstalk between oxidative stress and ferroptosis/oxytosis in ischemic stroke: possible targets and molecular mechanisms, Oxid. Med. Cell. Longev. 2021 (2021) 6643382, https://doi.org/10.1155/2021/6643382.
[7] X. Hu, et al., The role of ferroptosis and its mechanism in ischemic stroke, Exp. Neurol. 372 (2024) 114630, https://doi.org/10.1016/j.expneurol.2023.114630.
[8] W. Fan, et al., NRF2 activation ameliorates blood-brain barrier injury after cerebral ischemic stroke by regulating ferroptosis and inflammation, Sci. Rep. 14 (1) (2024) 5300, https://doi.org/10.1038/s41598-024-53836-0.
[9] A.K. Erdemoglu, et al., Serum ferritin levels and early prognosis of stroke, Eur. J. Neurol. 9 (6) (2002) 633–637, https://doi.org/10.1046/j.1468-1331.2002.00472.x.
[10] T. Grubić Kezele, et al., Age-related changes and sex-related differences in brain iron metabolism, Nutrients 12 (9) (2020) 2601, https://doi.org/10.3390/nu12092601.
[11] J. Chen, et al., Inhibition of acyl-CoA synthetase long-chain family member 4 facilitates neurological recovery after stroke by regulation ferroptosis, Front. Cell. Neurosci. 15 (2021) 632354, https://doi.org/10.3389/fncel.2021.632354.
[12] X. Jiang, et al., Ferroptosis: mechanisms, biology and role in disease, Nat. Rev. Mol. Cell Biol. 22 (4) (2021) 266–282, https://doi.org/10.1038/s41580-020-00324-8.
[13] Z. Kou, et al., Aryl hydrocarbon receptor: its roles in physiology, Biochem. Pharmacol. 185 (2021) 114428, https://doi.org/10.1016/j.bcp.2021.114428.
[14] A.S. Ganapathy, et al., Alpha-tocopherylquinone differentially modulates claudins to enhance intestinal epithelial tight junction barrier via AhR and Nrf2 pathways, Cell Rep. 42 (7) (2023) 112705, https://doi.org/10.1016/j.celrep.2023.112705.
[15] A.A. Tuz, et al., Ischemic stroke and concomitant gastrointestinal complications-a fatal combination for patient recovery, Front. Immunol. 13 (2022) 1037330, https://doi.org/10.3389/fimmu.2022.1037330.
[16] D. Guo, et al., Prognostic metrics associated with inflammation and atherosclerosis signaling evaluate the burden of adverse clinical outcomes in ischemic stroke patients, Clin. Chem. 66 (11) (2020) 1434–1443, https://doi.org/10.1093/clinchem/hvaa201.
[17] K. Xu, et al., Rapid gut dysbiosis induced by stroke exacerbates brain infarction in turn, Gut (2021) 2020–32363, https://doi.org/10.1136/gutjnl-2020-323263.
[18] E.A. Mayer, et al., The gut-brain Axis, Annu. Rev. Med. 73 (2022) 439–453, https://doi.org/10.1146/annurev-med-042320-014032.
[19] J. Liu, et al., Microbiota-microglia crosstalk between Blautia producta and neuroinflammation of Parkinson's disease: a bench-to-bedside translational approach, Brain Behav. Immun. 117 (2024) 270–282, https://doi.org/10.1016/j.bbi.2024.01.010.
[20] P.D. Cani, et al., Akkermansia muciniphila: paradigm for next-generation beneficial microorganisms, Nature reviews, Gastroenterol. Hepatol. 19 (10) (2022) 625–637, https://doi.org/10.1038/s41575-022-00631-9.
[21] C. Martin-Gallausiaux, et al., Akkermansia muciniphila upregulates genes involved in maintaining the intestinal barrier function via ADP-heptose-dependent activation of the ALPK1/TIFA pathway, Gut Microbes 14 (1) (2022) 2110639, https://doi.org/10.1080/19490976.2022.2110639.
[22] Y. Chang, et al., Microbiota dysbiosis and functional outcome in acute ischemic stroke patients, Sci. Rep. 11 (1) (2021) 10977, https://doi.org/10.1038/s41598-021-90463-5.
[23] K. Li, et al., Intestinal Akkermansia muciniphila is beneficial to functional recovery following ischemic stroke, J. Neuroimmune Pharmacol. 19 (1) (2024) 43, https://doi.org/10.1007/s11481-024-10146-6.
[24] Z. Lian, et al., Gut microbiota-derived melatonin from Puerariae Lobatae Radix-resistant starch supplementation attenuates ischemic stroke injury via a positive microbial co-occurrence pattern, Pharmacol. Res. 190 (2023) 106714, https://doi.org/10.1016/j.phrs.2023.106714.
[25] X. Liu, et al., Polymannuronic acid prebiotic plus Lacticaseibacillus rhamnosus GG probiotic as a novel synbiotic promoted their separate neuroprotection against Parkinson's disease, Food Res. Int. 155 (2022) 111067, https://doi.org/10.1016/j.foodres.2022.111067.
[26] E.Z. Longa, et al., Reversible middle cerebral artery occlusion without craniectomy in rats, Stroke 20 (1) (1989) 84–91, https://doi.org/10.1161/01.Str.20.1.84.
[27] Y. Luo, et al., Akkermansia muciniphila prevents cold-related atrial fibrillation in rats by modulation of TMAO induced cardiac pyroptosis, EBioMedicine 82 (2022) 104087, https://doi.org/10.1016/j.ebiom.2022.104087.
[28] S. Xie, et al., Novel tripeptide RKH derived from Akkermansia muciniphilaprotects against lethal sepsis, Gut 73 (1) (2024) 78–91, https://doi.org/10.1136/gutjnl-2023-329996.
[29] F.L. Zhang, et al., Microbiota-derived tryptophan metabolites indole-3-lactic acid is associated with intestinal ischemia/reperfusion injury via positive regulation of YAP and Nrf2, J. Transl. Med. 21 (1) (2023) 264, https://doi.org/10.1186/s12967-023-04109-3.
[30] Y. Jia, et al., Tetrandrine enhances the ubiquitination and degradation of Syk through an AhR-c-src-c-Cbl pathway and consequently inhibits osteoclastogenesis and bone destruction in arthritis, Cell Death Dis. 10 (2) (2019) 38, https://doi.org/

10.1038/s41419-018-1286-2.
[31] R.A. Swanson, et al., A semiautomated method for measuring brain infarct volume, J. Cerebr. Blood Flow Metabol. : Off. J. Int. Soc. Cerebr. Blood Flow Metabol. 10 (2) (1990) 290–293, https://doi.org/10.1038/jcbfm.1990.47.
[32] Y. Jiang, et al., Piezo 1 regulates intestinal epithelial function by affecting the tight junction protein claudin-1 via the ROCK pathway, Life Sci. 275 (2021) 119254, https://doi.org/10.1016/j.lfs.2021.119254.
[33] Y. Sun, et al., Parabacteroides distasonis ameliorates insulin resistance via activation of intestinal GPR109a, Nat. Commun. 14 (1) (2023) 7740, https://doi.org/10.1038/s41467-023-43622-3.
[34] J.F. Cryan, et al., The microbiota-gut-brain Axis, Physiol. Rev. 99 (4) (2019) 1877–2013, https://doi.org/10.1152/physrev.00018.2018.
[35] Y. Xia, et al., Lactobacillus-derived indole-3-lactic acid ameliorates colitis in cesarean-born offspring via activation of aryl hydrocarbon receptor, iScience 26 (11) (2023) 108279, https://doi.org/10.1016/j.isci.2023.108279.
[36] L. Zhao, et al., Bidirectional gut-brain-microbiota axis as a potential link between inflammatory bowel disease and ischemic stroke, J. Neuroinflammation 15 (1) (2018) 339, https://doi.org/10.1186/s12974-018-1382-3.
[37] J. Zhang, et al., Role of the gut microbiota in complications after ischemic stroke, Front. Cell. Infect. Microbiol. 14 (2024) 1334581, https://doi.org/10.3389/fcimb.2024.1334581.
[38] Y.H. Wang, et al., Prophylactic use of probiotics as an adjunctive treatment for ischemic stroke via the gut-spleen-brain axis, Brain Behav. Immun. 123 (2024) 784–798, https://doi.org/10.1016/j.bbi.2024.10.026.
[39] Z. Rahman, et al., Multistrain probiotics with fructooligosaccharides improve middle cerebral artery occlusion-driven neurological deficits by revamping microbiota-gut-brain Axis, Probiotics Antimicrob. Proteins 16 (4) (2024) 1251–1269, https://doi.org/10.1007/s12602-023-10109-y.
[40] C. Menjivar, et al., Akkermansia muciniphila, Trends Microbiol. (2024) 1143–1144, https://doi.org/10.1016/j.tim.2024.08.010.
[41] J.P. Ouwerkerk, et al., Complete genome sequence of Akkermansia glycaniphila strain PytT, a mucin-degrading specialist of the reticulated Python gut, Genome Announc. 5 (1) (2017), e01098 https://doi.org/10.1128/genomeA.01098-16, 16.
[42] B. Shuoker, et al., Sialidases and fucosidases of Akkermansia muciniphila are crucial for growth on mucin and nutrient sharing with mucus-associated gut bacteria, Nat. Commun. 14 (1) (2023) 1833, https://doi.org/10.1038/s41467-023-37533-6.
[43] X. Liu, et al., Transcriptomics and metabolomics reveal the adaption of Akkermansia muciniphila to high mucin by regulating energy homeostasis, Sci. Rep. 11 (1) (2021) 9073, https://doi.org/10.1038/s41598-021-88397-z.
[44] T. Zhang, et al., Akkermansia muciniphila is a promising probiotic, Microb. Biotechnol. 12 (6) (2019) 1109–1125, https://doi.org/10.1111/1751-7915.13410.
[45] V.F. Rodrigues, et al., Akkermansia muciniphila and gut immune system: a good friendship that attenuates inflammatory bowel disease, obesity, and diabetes, Front. Immunol. 13 (2022) 934695, https://doi.org/10.3389/fimmu.2022.934695.
[46] J. Liu, et al., Live and pasteurized Akkermansia muciniphila decrease susceptibility to Salmonella Typhimurium infection in mice, J. Adv. Res. 52 (2023) 89–102, https://doi.org/10.1016/j.jare.2023.03.008.
[47] H. Wade, et al., Akkermansia muciniphila and its membrane protein ameliorates intestinal inflammatory stress and promotes epithelial wound healing via CREBH and miR-143/145, J. Biomed. Sci. 30 (1) (2023) 38, https://doi.org/10.1186/s12929-023-00935-1.
[48] P. Nighot, et al., Endocytosis of intestinal tight junction proteins: in time and space, Inflamm. Bowel Dis. 27 (2) (2021) 283–290, https://doi.org/10.1093/ibd/izaa141.
[49] L.W. Kaminsky, et al., IL-1β and the intestinal epithelial tight junction barrier, Front. Immunol. 12 (2021) 767456, https://doi.org/10.3389/fimmu.2021.767456.
[50] G. Anogianakis, et al., Current trends in stroke biomarkers: the prognostic role of S100 calcium-binding protein B and glial fibrillary acidic protein, Life 14 (10) (2024) 1247, https://doi.org/10.3390/life14101247.
[51] N. Scherbakov, et al., Body weight changes and incidence of cachexia after stroke, J. Cachexia Sarcopenia Muscle 10 (3) (2019) 611–620, https://doi.org/10.1002/jcsm.12400.
[52] Y. Kim, et al., Prognostic importance of weight change on short-term functional outcome in acute ischemic stroke, Int. J. Stroke : Off. J. Int. Stroke Society 10 (Suppl A100) (2015) 62–68, https://doi.org/10.1111/ijs.12554.
[53] D.T. Winovich, et al., Factors associated with ischemic stroke survival and recovery in older adults, Stroke 48 (7) (2017) 1818–1826, https://doi.org/10.1161/strokeaha.117.016726.
[54] N.M. Maftei, et al., The potential impact of probiotics on human health: an update on their health-promoting properties, Microorganisms 12 (2) (2024) 234, https://doi.org/10.3390/microorganisms12020234.
[55] J. Suez, et al., The pros, cons, and many unknowns of probiotics, Nat. Med. 25 (5) (2019) 716–729, https://doi.org/10.1038/s41591-019-0439-x.
[56] W. Deng, et al., Gut metabolites acting on the gut-brain Axis: regulating the functional state of microglia, Aging Dis. 15 (2) (2024) 480–502, https://doi.org/10.14336/ad.2023.0727.
[57] A. Wang, et al., Indole-3-Lactic acid, a tryptophan metabolite of lactiplantibacillus plantarum DPUL-S164, improved intestinal barrier damage by activating AhR and Nrf2 signaling pathways, J. Agric. Food Chem. 71 (48) (2023) 18792–18801, https://doi.org/10.1021/acs.jafc.3c06183.
[58] C.B. Wong, et al., Potential effects of indole-3-lactic acid, a metabolite of human bifidobacteria, on NGF-induced neurite outgrowth in PC12 cells, Microorganisms 8 (3) (2020) 398, https://doi.org/10.3390/microorganisms8030398.
[59] Q. Zhang, et al., Lactobacillus plantarum-derived indole-3-lactic acid ameliorates colorectal tumorigenesis via epigenetic regulation of CD8(+) T cell immunity, Cell Metab. 35 (6) (2023) 943–960.e9, https://doi.org/10.1016/j.cmet.2023.04.015.
[60] X. Qian, et al., Bifidobacteria with indole-3-lactic acid-producing capacity exhibit psychobiotic potential via reducing neuroinflammation, Cell Rep. Med. 5 (11) (2024) 101798, https://doi.org/10.1016/j.xcrm.2024.101798.
[61] J. Xie, et al., Akkermansia muciniphila protects mice against an emerging tick-borne viral pathogen, Nat. Microbio. 8 (1) (2023) 91–106, https://doi.org/10.1038/s41564-022-01279-6.
[62] A.Y. Grishanova, et al., Aryl hydrocarbon receptor in oxidative stress as a double agent and its biological and therapeutic significance, Int. J. Mol. Sci. 23 (12) (2022) 6719, https://doi.org/10.3390/ijms23126719.
[63] X. Deng, et al., Nrf2 and ferroptosis: a new research direction for ischemic stroke, Cell. Mol. Neurobiol. 43 (8) (2023) 3885–3896, https://doi.org/10.1007/s10571-023-01411-y.
[64] J. Guo, et al., Iron, ferroptosis, and ischemic stroke, J. Neurochem. 165 (4) (2023) 487–520, https://doi.org/10.1111/jnc.15807.
[65] Y. Sun, et al., Gut firmicutes: relationship with dietary fiber and role in host homeostasis, Crit. Rev. Food Sci. Nutr. 63 (33) (2023) 12073–12088, https://doi.org/10.1080/10408398.2022.2098249.
[66] M.K. Yadav, et al., Probiotics, prebiotics and synbiotics: safe options for next-generation therapeutics, Appl. Microbiol. Biotechnol. 106 (2) (2022) 505–521, https://doi.org/10.1007/s00253-021-11646-8.
[67] K.S. Swanson, et al., The International Scientific Association for Probiotics and Prebiotics (ISAPP) consensus statement on the definition and scope of synbiotics, Nature reviews, Gastroenterol. Hepatol. 17 (11) (2020) 687–701, https://doi.org/10.1038/s41575-020-0344-2.
[68] G.R. Gibson, et al., Expert consensus document: the International Scientific Association for Probiotics and Prebiotics (ISAPP) consensus statement on the definition and scope of prebiotics, Nature reviews, Gastroenterol. Hepatol. 14 (8) (2017) 491–502, https://doi.org/10.1038/nrgastro.2017.75.
[69] C. Wang, et al., A synbiotic formulation of Lactobacillus reuteri and inulin alleviates ASD-like behaviors in a mouse model: the mediating role of the gut-brain axis, Food Funct. 15 (1) (2024) 387–400, https://doi.org/10.1039/d3fo02663a.